

### 3.6 Pavement Performance

#### 3.6.1 Vertical Displacement

Vertical displacement of the slabs was measured at about 25.4 cm (10 in) from each side of the joints, in both the steel dowel slab and the FRP slab. Displacement tests were conducted before applying any load (at zero repetition) and every 200,000 repetitions afterwards up to one million repetitions. Displacement measurements were made in order to draw load/deflection curves. For these tests, the fatigue cyclic loads were stopped, and static loads were applied in 5,000 lbs increments up to a maximum axle load of 40,000 lbs. The four dial indicators with 0.001" accuracy shown in Figure 3.7 were read and recorded manually. One load/deflection curve was drawn from each gage reading. When the east beam was loaded (east loading), gages 1 and 3 were considered "under load" (or on the loaded slab) and gages 2 and 4 were considered "across load" or (across from the loaded slab). This is the opposite when the west beam was loaded (west loading). A typical load/deflection curve is shown in Figure 3.10 from gage No. 1 for the case of east loading, after the first 200,000 cycles were applied.

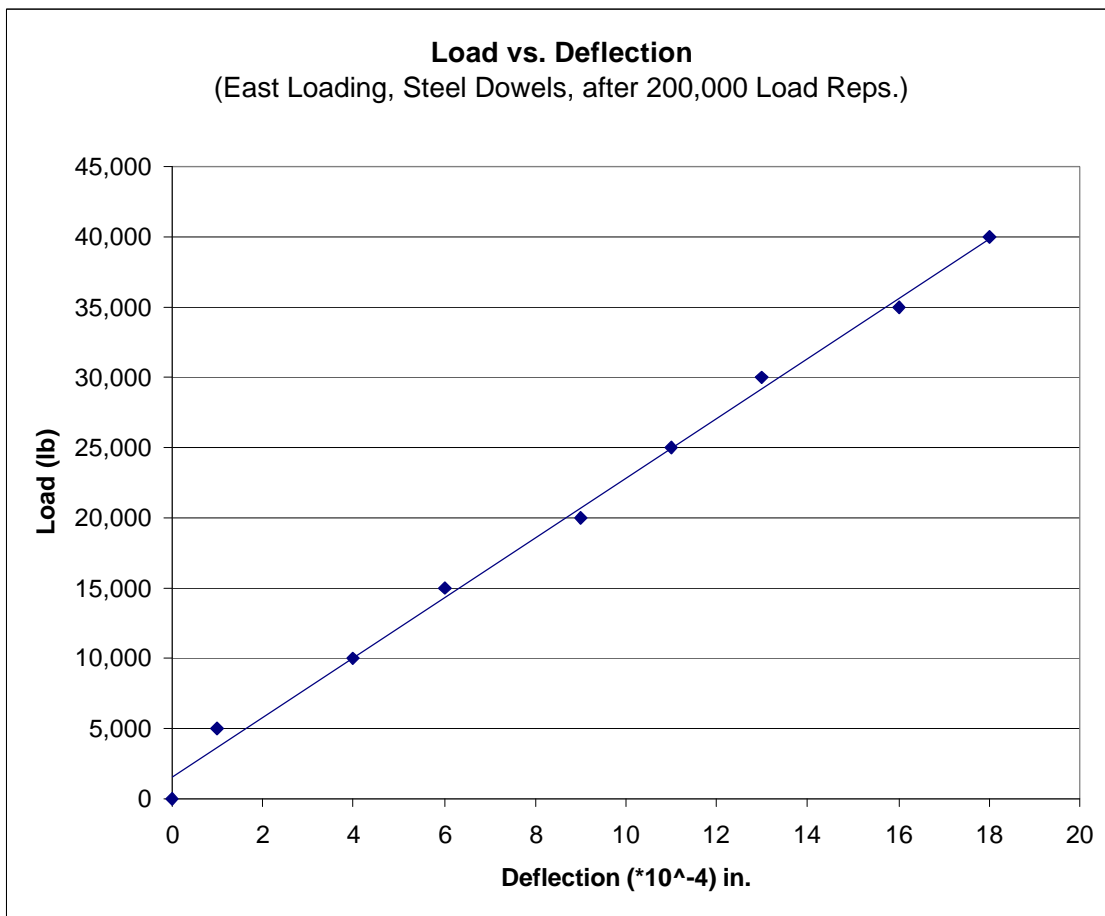


Figure 3.10 Load vs. Deflection After 200,000 Cycles  
(Measurement from Gage 1)

The slope of the load/deflection curve is an indication of the stiffness of the slab since stiffness  $k$  is defined as the ratio of the load  $P$  over the displacement  $d$ . The variation of the slope (stiffness) was correlated against the number of load cycles applied to the specimens. This is shown in Figure 3.11 which gives the data points and linear regression lines for the east and west loading, with the steel and FRP dowels side-by-side. For all cases, it can be shown that the slope increases as the number of load applications increases. Such an increase in slope signifies that for a given level of loading the corresponding vertical displacement is reduced. Normally one would expect vertical displacements to increase as the number of cycles increases and the specimen weakens or experiences damage. In this case, the decreased deflection (and consequently increase in slope) can be attributed to the additional compaction of the soil and not to a reduction in stiffness.

### **3.6.2 Load Transfer Efficiency**

The load transfer efficiency (LTE) was calculated using the slopes (stiffness) from the load/displacement data. For this experiment, LTE is defined as the ratio of the loaded to non-loaded slopes from the load/deflection curves. The load deflection curves were developed by loading one side of the joint while measuring the corresponding deflections from the loaded and non-loaded sides of the joint. A value of LTE larger than 100% indicates a “frozen” (or rigid) joint. A value slightly greater than 100% may be attributed to a human error (reading/recording) or improper zeroing of the gages. The variation of the load transfer efficiency with the number of load cycles applied is shown in Figure 3.12.

By examining the graphs in Figure 3.12, it can be seen that, except for the case of east loading with steel dowels, the LTE is generally reduced as more cycles are applied to the pavement. This was to be expected since the joints should weaken or deteriorate over time and under service loads. It can also be noted that the magnitude of the LTE is smaller in the FRP joints, and that the decrease in the LTE over time is more rapid than in the steel joints.

### **3.6.3 Joint Movement**

The horizontal movement of the joint was measured using the dial indicators (one on each specimen). These measurements were read and manually recorded at the beginning of the experiment and after every 100,000 load repetitions. Because of the cyclic temperature change, the joint opened and closed a considerable amount. The results are shown in Tables 3.1 through 3.3. Positive movement (+) indicates joint closing due to heating or slab expansion, and negative movement (-) indicates joint opening from cooling or slab contraction.

By observing the data obtained, it can be seen that 100 percent of the time, the FRP joint shows more movement than the steel joints during heating (or joint closing). However, the joint built with steel dowels had more movement 80 percent of the time, during cooling (or joint opening). It should be noted that the magnitude of these joint movements is not cumulative. In other words, the dial indicators were installed and zeroed out at the end of a working the day after 100,000 cycles have been applied and read and then removed the next morning when testing was about to begin.

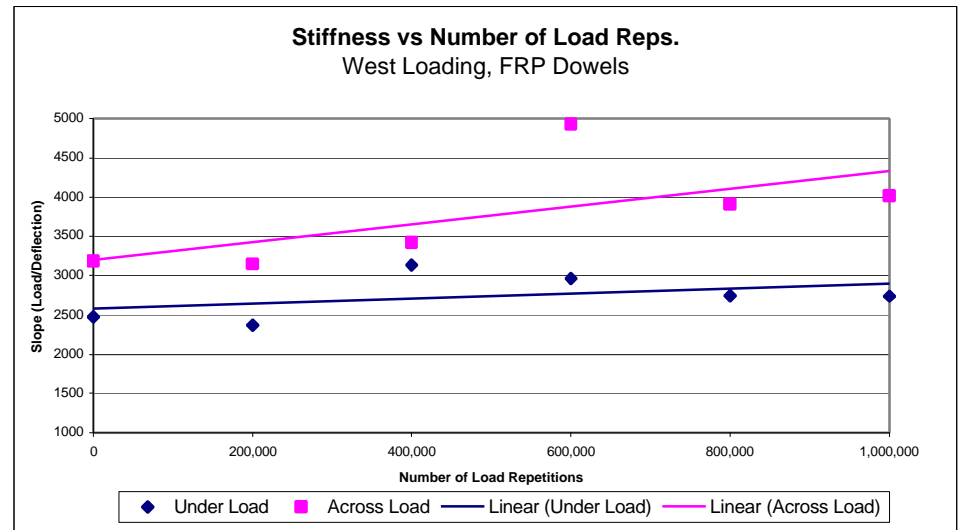
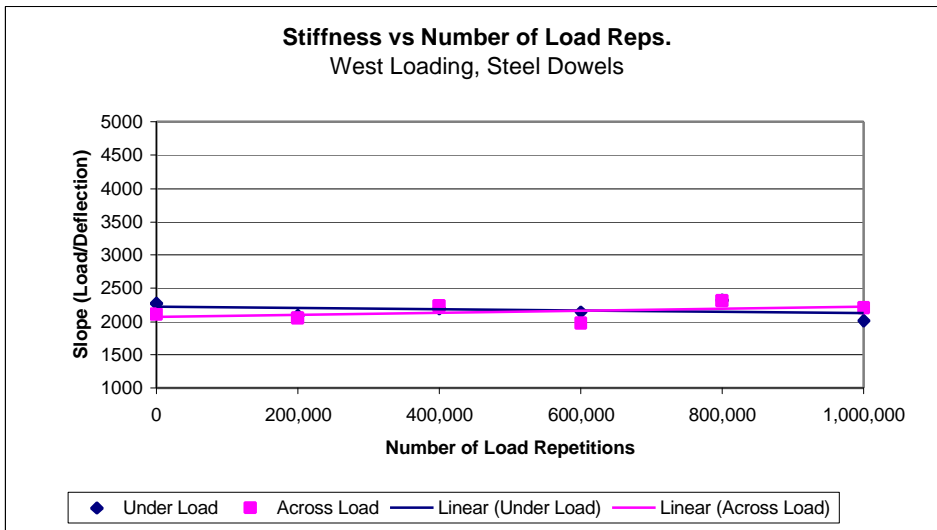
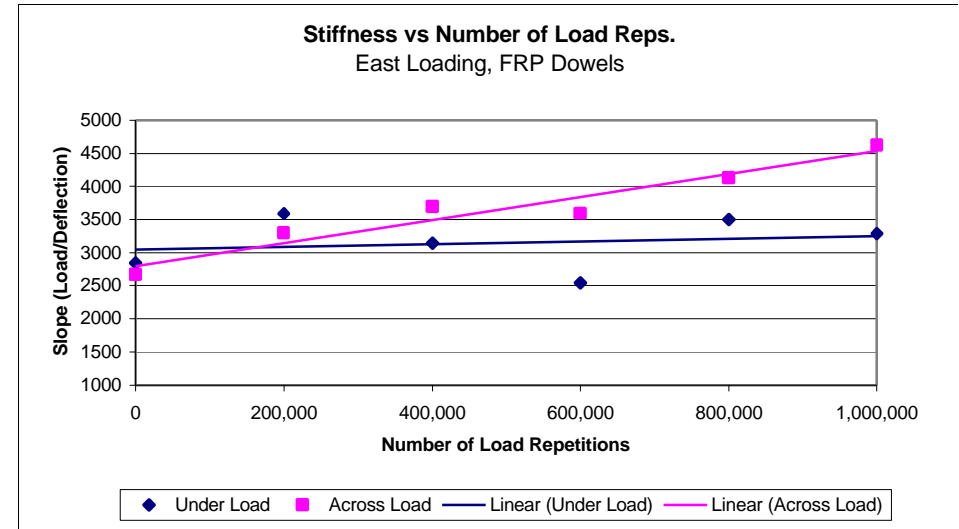
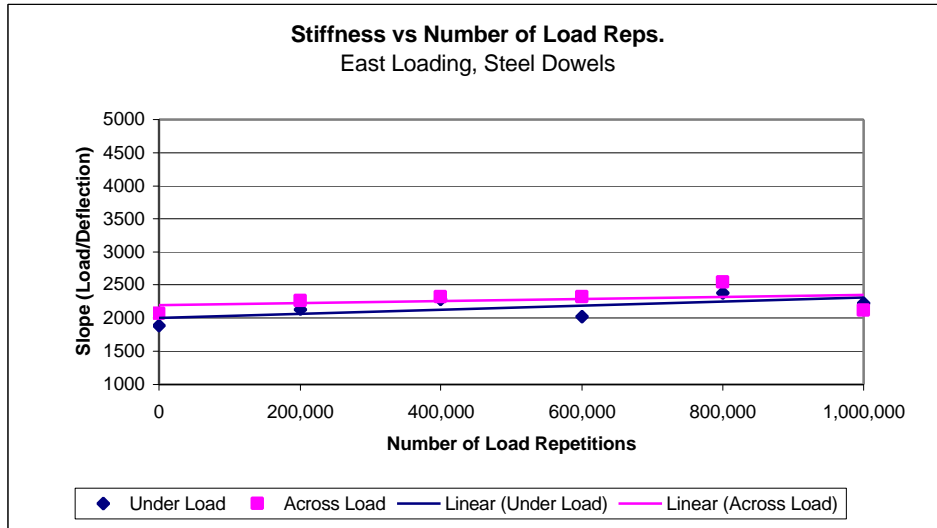


Figure 3.11 Comparing Stiffness of Steel and FRP Dowels

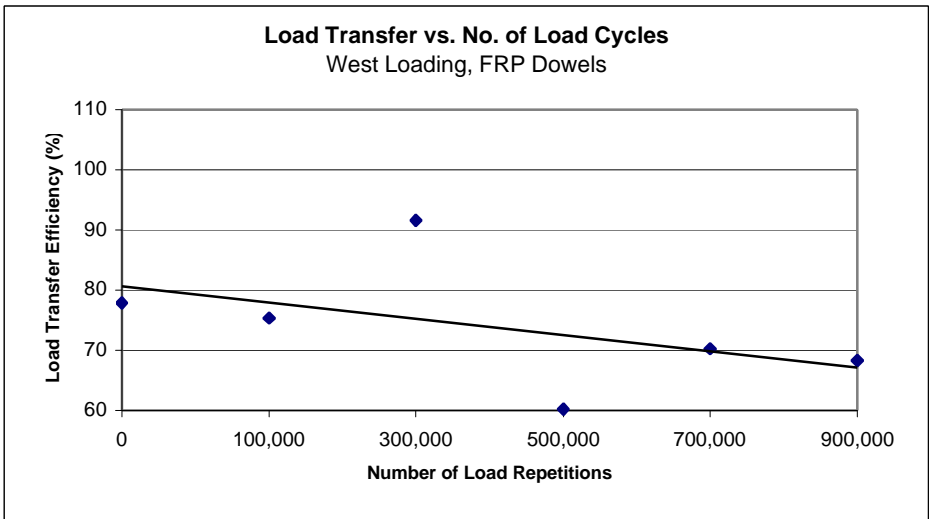
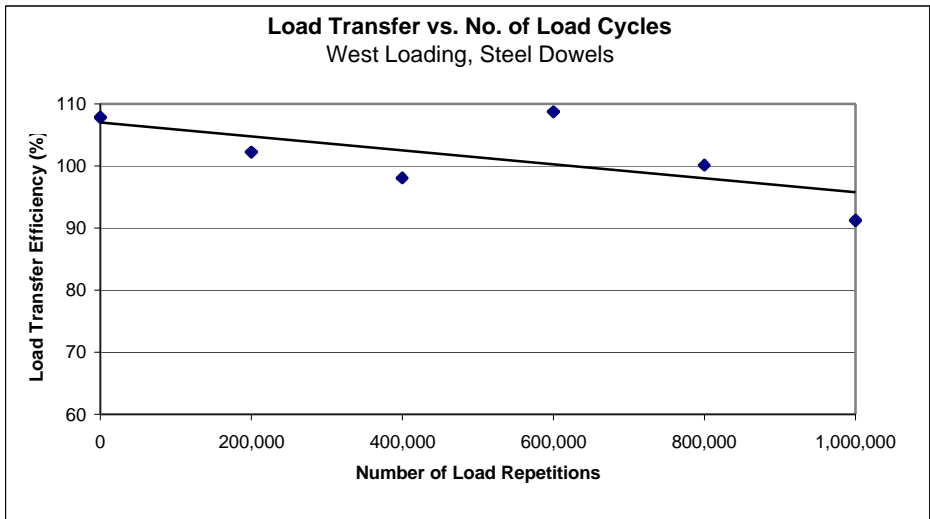
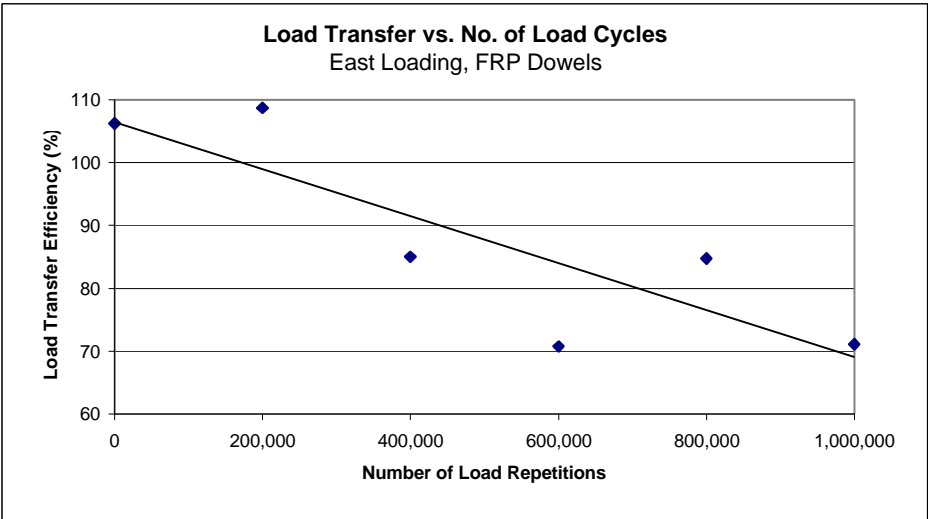
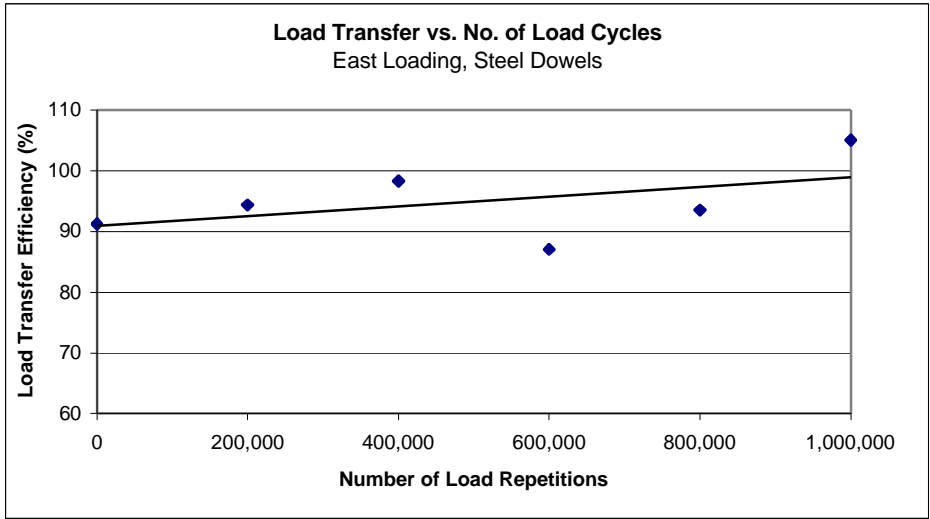


Figure 3.12 Variation of Load Transfer Efficiency with Respect to Number of Load Cycles

Table 3.1 Measured Joint Movement Due to Change in Temperature

| Heating / Cooling Cycle |   |        |       |                                       |        |      | Joint Movement |                             |                           |
|-------------------------|---|--------|-------|---------------------------------------|--------|------|----------------|-----------------------------|---------------------------|
| No. of Load Reps.       | Start temp. (°F)<br>(approx. 4:00 p.m.) |        |       | End temp. (°F)<br>(approx. 9:00 a.m.) |        |      | ΔT<br>(°F)     | Steel<br>x 10 <sup>-4</sup> | FRP<br>x 10 <sup>-4</sup> |
|                         | Top                                     | Bottom | Avg.  | Top                                   | Bottom | Avg. |                |                             |                           |
|                         | Concrete Curing / Settling (Cooling)    |        |       |                                       |        |      |                | -30                         | -30                       |
| 0                       | 75                                      | 75     | 75    | 110                                   | 90     | 100  | 25             | 60                          | 60                        |
| 100,000                 | 110                                     | 91     | 100.5 | 83                                    | 85     | 84   | -16.5          | -33                         | -19                       |
| 200,000                 | 81                                      | 83     | 82    | 47                                    | 74     | 60.5 | -21.5          | -20                         | -10                       |
| 300,000                 | 53                                      | 74     | 63.5  | 75                                    | 75     | 75   | 11.5           | 4                           | 17                        |
| 400,000                 | 75                                      | 75     | 75    | 103                                   | 83     | 93   | 18             | 24                          | 40                        |
| 500,000                 | 109                                     | 88     | 98.5  | 78                                    | 83     | 80.5 | -18            | -19                         | -44                       |
| 600,000                 | 84                                      | 83     | 83.5  | 47                                    | 73     | 60   | -23.5          | -48                         | -27                       |
| 700,000                 | 42                                      | 71     | 56.5  | 75                                    | 75     | 75   | 18.5           | 23                          | ---                       |
| 800,000                 | 74                                      | 75     | 74.5  | 105                                   | 86     | 95.5 | 21             | 34                          | 51                        |
| 900,000                 | 108                                     | 88     | 98    | 74                                    | 79     | 76.5 | -21.5          | -38                         | -27                       |

Note: (+) indicates an increase in temp. (heating) and joint closing  
 (-) indicates a decrease in temp. (cooling) and joint opening

Table 3.2 Measured Joint Movement Due to Change in Temperature

| Heating / Joint Closing   |            |                             |                           | Cooling / Joint Opening   |            |                             |                           |
|---------------------------|------------|-----------------------------|---------------------------|---------------------------|------------|-----------------------------|---------------------------|
| Total No. Of Reps applied | ΔT<br>(°F) | Joint Movement              |                           | Total No. of Reps applied | ΔT<br>(°F) | Joint Movement              |                           |
|                           |            | Steel<br>x 10 <sup>-4</sup> | FRP<br>x 10 <sup>-4</sup> |                           |            | Steel<br>x 10 <sup>-4</sup> | FRP<br>x 10 <sup>-4</sup> |
| 300,000                   | 11.5       | 4                           | 17                        | 100,000                   | -16.5      | -33                         | -19                       |
| 400,000                   | 18         | 24                          | 40                        | 200,000                   | -21.5      | -20                         | -10                       |
| 700,000                   | 18.5       | 23                          | ---                       | 500,000                   | -18        | -19                         | -44                       |
| 800,000                   | 21         | 34                          | 51                        | 600,000                   | -23.5      | -48                         | -27                       |
|                           |            |                             |                           | 900,000                   | -21.5      | -38                         | -27                       |

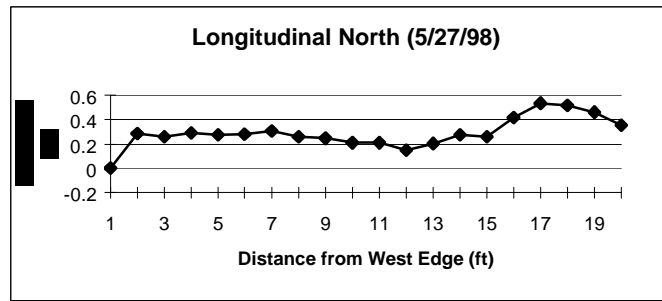
Table 3.3 Measured Joint Movement Due to Change in Temperature

| Total Number of Repetitions applied | ΔT (°F) | Heating / Joint Closing  |                        | Cooling / Joint Opening  |                        |
|-------------------------------------|---------|--------------------------|------------------------|--------------------------|------------------------|
|                                     |         | Steel x 10 <sup>-4</sup> | FRP x 10 <sup>-4</sup> | Steel x 10 <sup>-4</sup> | FRP x 10 <sup>-4</sup> |
| 100,000                             | -16.5   |                          |                        | -33                      | -19                    |
| 200,000                             | -21.5   |                          |                        | -20                      | -10                    |
| 300,000                             | 11.5    | 4                        | 17                     |                          |                        |
| 400,000                             | 18      | 24                       | 40                     |                          |                        |
| 500,000                             | -18     |                          |                        | -19                      | -44                    |
| 600,000                             | -23.5   |                          |                        | -48                      | -27                    |
| 700,000                             | 18.5    | 23                       | ---                    |                          |                        |
| 800,000                             | 21      | 34                       | 51                     |                          |                        |
| 900,000                             | -21.5   |                          |                        | -38                      | -27                    |

Although the values of the joint opening/closing are not very consistent, they indicate the joints were constructed properly and that they were performing their function as thermal expansion joints.

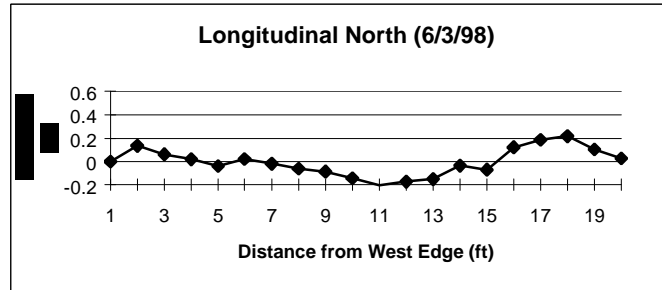
### 3.6.4 Slab Curling

As indicated in the monitoring plan of Figure 3.8, longitudinal profiles were constructed based on face dipstick measurements made on the exposed outer 0.610 m (2 ft) strips of the pavement slabs. The selection of the frequency at which the measurements were made was based on the requirement of having two sets or readings for each case of room temperature conditions, warm conditions (37.8°C or 100 °F), and cold condition (4.44°C or 40°F). The corrected profiles were plotted and are shown in Figure 3.13 for the north slab, and Figure 3.14 for the south slab.



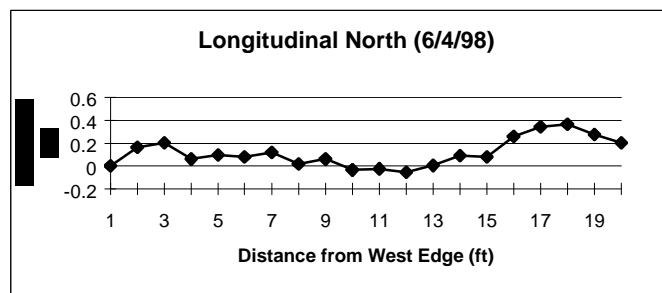
After

Avg. Surface Temp (F) =  
 Avg. Bottom Temp (F) =  
 Temp. Gradient =



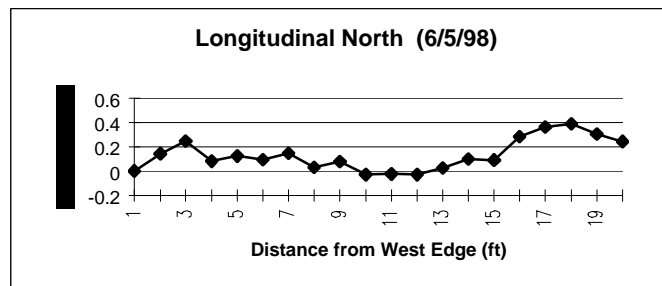
After

Avg. Surface Temp (F) =  
 Avg. Bottom Temp (F) =  
 Temp. Gradient =



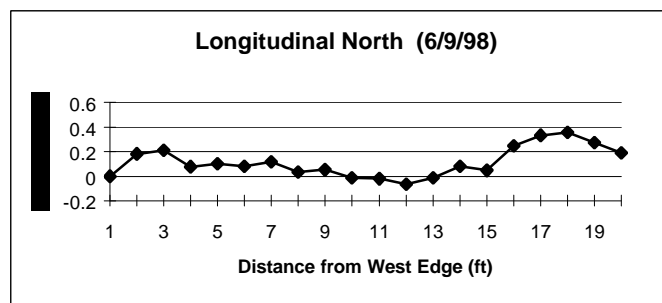
After

Avg. Surface Temp (F) =  
 Avg. Bottom Temp (F) =  
 Temp. Gradient =



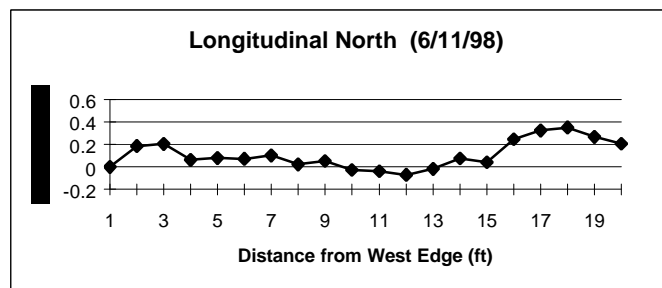
After

Avg. Surface Temp (F) =  
 Avg. Bottom Temp (F) =  
 Temp. Gradient =



After

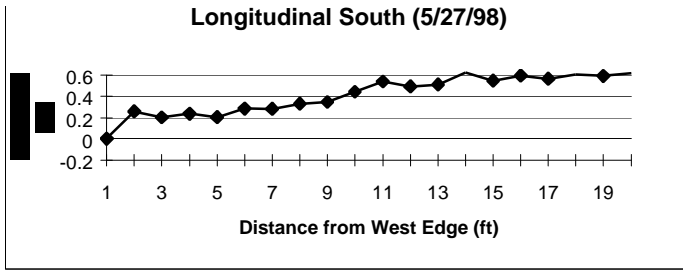
Avg. Surface Temp (F) =  
 Avg. Bottom Temp (F) =  
 Temp. Gradient =



After

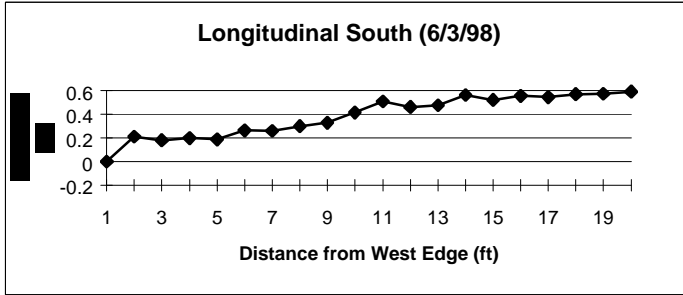
Avg. Surface Temp (F) =  
 Avg. Bottom Temp (F) =  
 Temp. Gradient =

Figure 3.13 North Profiles (Steel)



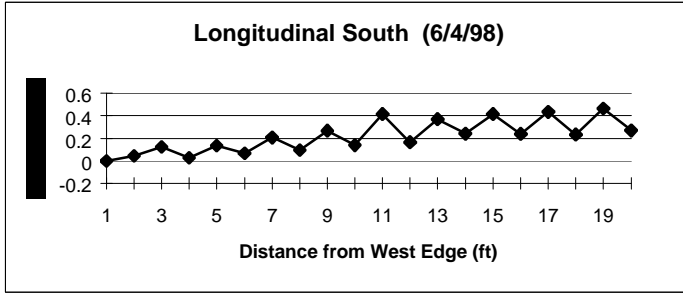
After  Load Reps

Avg. Surface Temp. (F) = 70  
 Avg. Bottom Temp. (F) = 70  
 Temp Gradient = 0



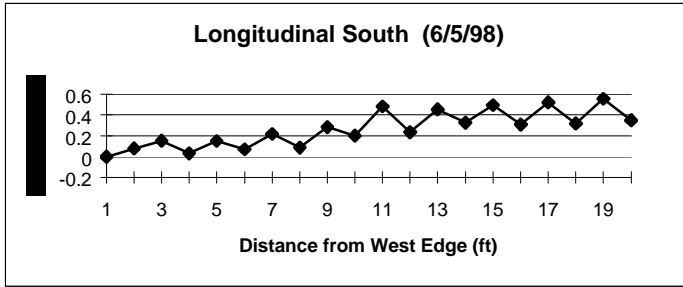
After  Load Reps

Avg. Surface Temp. (F) = 110  
 Avg. Bottom Temp. (F) = 90  
 Temp Gradient = 20



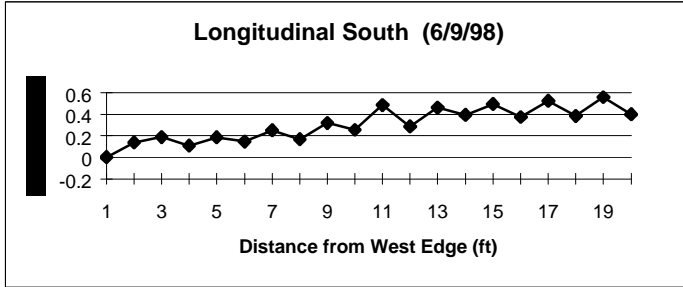
After  Load Reps

Avg. Surface Temp. (F) = 83  
 Avg. Bottom Temp. (F) = 85  
 Temp Gradient = 2



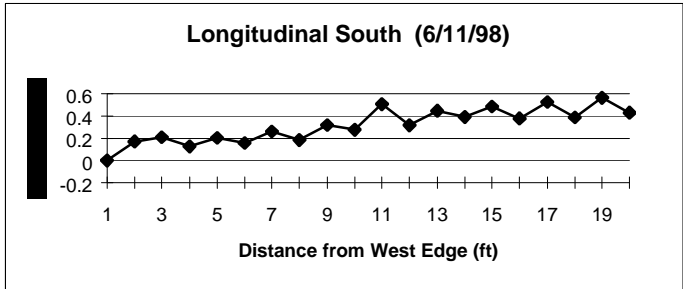
After  Load Reps

Avg. Surface Temp. (F) = 47  
 Avg. Bottom Temp. (F) = 74  
 Temp Gradient = 27



After  Load Reps

Avg. Surface Temp. (F) = 103  
 Avg. Bottom Temp. (F) = 83  
 Temp Gradient = 20



After  Load Reps

Avg. Surface Temp. (F) = 47  
 Avg. Bottom Temp. (F) = 73  
 Temp Gradient = 26

Figure 3.14 South Profiles (FRP)

## 3.7 Results and Conclusions

### 3.7.1 Test Results

At 1 million load repetitions, both slabs were still in good condition. Water was added to the subbase at the joints and testing continued for another day. After 1.1 million repetitions, a full-depth, full-width, crack developed in the slab with the steel dowels at a distance of about 0.914 m (3 ft) west from the joint line. Testing continued up to 2.2 million repetitions at which the broken slab deteriorated further with multiple other cracks, but the second slab (the one with FRP dowels) did not break. It was then decided to stop the load application and perform a detailed analysis on sections cut from both slabs around the joints. This analysis was done by KDOT and is summarized below.

### 3.7.2 Post Mortem Investigation

Square blocks (0.610 m by 0.610 m or 2 ft by 2 ft) were saw-cut through the full depth of the slabs around the joint line. Even though the slab with the steel dowels was cracked and the one with FRP dowels was not, both joints were in good condition since the cracks were way (.914 m or 3 ft) behind the joint line.

Two dowel bars from each of the steel and fiberglass slabs were examined. The specimens with steel bars were designated S1 and S2, and those with the FRP composite bars C1 and C2. A push-out test was conducted on each of the dowels. It consisted of exposing about 25.4 mm (1 in) of the bar at one end and the other end being flush with the concrete. Then the bars were loaded in a compression machine pushing on the exposed end of the bar and using a ring to support the concrete at the other end. The movement was limited to 3.18 mm (1/8 in.).

The peak load for the first steel bar (S1) was 10.61 kN (2386 lbf). The encased area of the bar was 156.6 cm<sup>2</sup> (24.27 in.<sup>2</sup>), therefore the push out stress is 676 kPa (98 psi). The bar was then re-pushed and a peak load of 2.56 kN (575 lbf) and a steady load of 2.34 kN (525 lbf) were obtained over 3.18 mm (1/8 in) displacement. The second specimen (S2) had its steel bar tack welded to the top chord of the wire basket. Therefore no valid test result was obtained on this bar. The peak load for the first composite bar (C1) was 4.56 kN (1026 lbf). The encased area is 224.9 cm<sup>2</sup> (34.86 in.<sup>2</sup>), therefore the push out stress is 200 kPa (29 psi). The second composite bar (C2) had a peak load of 7.57 kN (1702 lbf) and an encased area of 259.4 cm<sup>2</sup> (40.20 in.<sup>2</sup>), resulting in a push out stress of 290 kPa (42 psi).

Once the push-out tests were completed, the concrete was split through the long axis of the dowel (see Figure 3.15, a through d). It can be seen from the figure that the end of bar C2 was glued to its supporting stake with epoxy resin during construction, and therefore this half of the bar was not greased. However, the end bar C1 was not glued and consequently it constituted the half of the bar that was greased. This explains why C1 has a push-off stress of about 70% of that of C2. On the other hand comparing S1

and C1 (both greased) shows that the bond stress between steel and concrete is more than three times as much as the bond stress between the fiberglass and concrete (676 kPa (98 psi) compared to 200 kPa (29 psi)). This was expected because steel is known to have a bond to concrete that is superior to any other material with concrete.

As shown in the pictures, by splitting the concrete around the bars, it could be seen that the dowels were in good condition. No abrasions, striations, or chipped coating could be seen. The bars were firmly in place and no annular space was observed.

### **3.7.3 Conclusion**

From the results obtained, there does not seem to be considerable difference between the performance of the PCCP with steel dowels and that with FRP dowels. The change with time in deflection and load transfer efficiency, even though not the same between the two slabs, does not suggest any significant advantage of one type of dowels as opposed to the other. The fact that the slab with steel dowels cracked at 1.1 million load cycles and the one with FRP dowels did not crack even after the double number of cycles is not enough to draw a definite conclusion that FRP dowels are better than steel dowels. One test specimen of each type is not enough in experimental investigations and more replicates are usually necessary in experimental research, especially with Portland cement concrete structures.

It can be concluded however that the 38.1 mm (1.5 in.) FRP dowels can perform at least as good as the 25.4 mm (1 in.) steel dowels when subjected to cyclic loads across the PCCP joints. After 2.2 million cycles of a load equivalent to a 178 kN (40 kips) single axle, both types of dowels were in good condition. The thin layer of grease applied on half the dowels during construction reduces the bond stresses between the dowels and the concrete by about 30% but does not totally eliminate the bond.

The recommendations of this investigation to the highway and transportation agencies are to study and monitor the performance of test sections built in the field with FRP dowels and additional experimental studies performed by the different states and universities. Table 3.4 indicates various locations where field testing is performed on FRP dowels bars. It is also recommended to perform a couple of similar tests at the K-ATL to determine if the failure would be consistent with this experiment or if it was just a singular case.



Figure 3.15 (a) and (b) Steel Push-Out Test Specimens



Figure 3.15 (c) and (d) Steel Push-Out Test Specimens

Table 3.4 Summary of Plan, Schedule, Sites and Tests for Field Program. FRP and Stainless Steel dowel HITEC Evaluation. May 6, 1998. (Adapted from HITEC, 1998)

| Location  | Timing    | Materials       | Tests / Observations   |
|-----------|-----------|-----------------|--|
| ILLINOIS  | 1997      | FRP             | Construction costs & features<br>FWD load transfer<br>Faulting   |
|           | 1998      | Stainless & FRP | Dowel position check<br>Concrete cracks & spalls<br>Traffic loading data   |
| IOWA      | 1997      | Stainless & FRP | Construction costs & features<br>FWD load transfer<br>Faulting<br>Dowel position check<br>Concrete cracks & spalls<br>Traffic loading data                                 |
| KANSAS    | 10/01/97  | FRP             | Construction costs & features<br>FWD load transfer<br>Faulting<br>Dowel position check<br>Concrete cracks & spalls<br>Traffic loading data                                 |
| OHIO      | 10/16/97  | Stainless & FRP | Construction costs & features<br>FWD load transfer<br>Faulting<br>Dowel position check<br>Concrete cracks & spalls<br>Traffic loading data                                 |
|           | Fall 1997 |                 | FWD tests at joints<br>GPR dowel position verification<br>Inspection of joint conditions<br>Core 3 dowels, each mat'l and cutout<br>3 full dowels, each mat'l at each site |
| WISCONSIN | Fall 1997 | Stainless & FRP | Construction costs & features<br>FWD load transfer<br>Faulting<br>GPR dowel position check<br>Concrete cracks & spalls<br>Traffic loading data                             |

## **4.0 COMPARISON OF A 203 mm (8 in) AC WITH 127 mm (5 in) AC ON 127 mm (5 in) RAP Pavement Section**

This chapter describes the first experiment performed under the Fiscal Year 98 contract (ATL-98-1), which is the fifth experiment conducted at the facility (ATL-Exp#5). This experiment was funded by the Midwest Accelerated Pooled Fund study. This is the first experiment in which asphalt strain gauges and soil pressure cells were placed to record and monitor pavement performance.

The purpose of this experiment is to compare the performance of a full depth asphaltic concrete (AC) pavement placed directly on the subgrade with a reduced depth of this asphaltic concrete on a base layer of AC milling, on the same subgrade. Testing was performed in the middle (large) pit of the K-ATL using the rolling wheel/axle load assembly. Two lanes were placed side-by-side in this pit and tested simultaneously.

### **4.1 Pavement Structure**

The pavement structure consists of two 2.44 m (8 ft)-wide lanes side-by-side. The first lane was a 203 mm (8 in.) layer of asphaltic concrete on fine grained silt-clay subgrade and was placed in the north half of the pit. The second lane was 127 mm (5 in.) of asphaltic concrete on 127 mm (5 in.) of asphaltic concrete millings with fine grained subgrade, and was placed in the south half of the pit. The outer edges of the slabs were kept free since there was about a 0.610 m (2 ft) distance between the edges of the slabs and the north and south walls of the pit.

The 50-blow Marshall mix design was prepared at the Asphalt Material Lab at KSU under the direction of Professor Hossain. It is a TYPE 14 NDOR Mix using Gradation Band B and is shown in Appendix A. The mixture has a 30% Martin Marietta crushed limestones (CS-1), 15% 3/8-in. Dolese manufactured sand, 35% Kansas river sand and sand gravel, and 20% limestone screening. The design binder content corresponding to 4% air voids is 5.8%. The design was approved by the representative on the Technical Committee for the Nebraska Department of Roads who was also present during placement by the paving contractor.

### **4.2 Soil and Subgrade**

The subgrade for this experiment was the same as that of the ATL-97-1 experiment (ATL-Exp#3) since that was the last one in this pit preceding this current experiment. The soil is therefore the same as previously described in Section 2.2 except that there was no granular subbase. When the asphalt overlays (102 mm or 4 in.) of the test specimens of ATL-Exp#3 experiment were removed from the pit, the 229 mm (9 in.) PCCP slabs and the 102 mm (4 in.) of AB-3 granular subbase from the ATL-Exp#2 were removed as well. The soil level was then brought to about 330 mm (13 in.) below the floor level. New soil needed to be added to reach the required depth of 254 mm (10 in.) on the south lane and 203 mm (8 in.) on the north

lane. The silty clay soil added was close to the one originally used in the pit. The compaction test performed on this soil showed that a maximum dry density of  $1.63 \times 10^3 \text{ kg/m}^3$  (101.3 pcf) is obtained at the optimum moisture content of 19.4%.

### **4.3 Testing Conditions**

The middle (large) pit of the K-ATL was used for this experiment. Both slabs, the full depth without base and the reduced depth on a RAP base, were tested side-by-side such that the load was applied simultaneously on both. Half the axle (a pair of wheels) was running on one slab while the second half was on the other.

#### **4.3.1 Load Application**

A standard single axle of 80 kN (18,000 lbs) with dual tires at air pressure of 620 kPa (90 psi) was used to apply the load repetitions. In order to use only one axle of the truck bogie, pressure was disconnected from the suspension air-bags of the west axle, and this axle was lifted up and tied with chains so that it does not get in contact with the pavement at all. Therefore, only the east axle was in contact with the surface of the pavement. This resulted in a not-perfectly-symmetric operation because this single axle (not at the center of the carriage, but eccentric to the east) will hit the pavement sooner when traveling from West to East than when traveling from East to West. This could be one of the reasons why strain and pressure readings were not exactly the same on the east and west halves of the slabs.

The load application was in two directions, i.e. on both paths of each cycle of the wheel carriage. The travel was on a fixed path in the sense that no wheel wandering was simulated.

#### **4.3.2 Temperature Application**

The original experiment design called for testing to be conducted in a summer environment of 32°C (90°F). The infrared radiant heaters were to be used for this purpose; however, since the asphalt mix placed was found to be softer than anticipated, it was decided not to apply any additional heat to the surface. Also, testing was done during the month of August when the ambient temperature in the Lab throughout most of the day was around 32°C (90°F), and sometimes even higher. The temperatures would somewhat drop in the evenings and during the night, but load application was always done during the day. In general, during testing, the temperature of the pavement surface did not go below or above 32°C (90°F) by more than a few degrees.

## 4.4 Experiment Monitoring

This section describes the different types of instrumentation used to record the pavement behavior and the plan followed to monitor its performance.

### 4.4.1 Instrumentation

To compare the performance of the two pavement slabs the following instrumentation was used:

1. Strain Gauges,
2. Thermocouples,
3. Soil pressure cells, and
4. Moisture Sensors.

The location of the different sensors is shown in Figure 4.1. In addition to measurements obtained from these sensors, FWD tests were conducted at the beginning of the experiment, and nuclear density measurements and surface profiles were recorded periodically.

Data were collected using a data acquisition system developed at Kansas State University during previous research contracts. This was augmented by some additional boards, modules, and computer upgrades. The new modules acquired were for reading the strain gauges and pressure cells. The system generally consists of several terminal blocks connected to a number of corresponding SCXII modules mounted on an instrumentation chassis. Data acquisition boards are installed in a PC computer with Pentium processors. The software consist of the LabView development package in which several program interfaces (Virtual Instruments, or V.I.'s) were implemented. All hardware and software are products of National Instruments, Inc.

#### 4.4.1.1 Strain Gauges

Six strain gauges, Model PAST-2AC (from Dynatest), were placed as indicated in Figure 4.1 along the centerline of each pair of wheels at the quarter-span points. The centerline of the wheel paths for the north and south lanes are symmetrically located at 991 mm (39 in.) from the middle of the pit. Three strain gauges were therefore placed on each wheel path. The gauges (often designated as H-gauges) consist of electrical resistors embedded within a strip of glass-fiber reinforced epoxy supported at each end of the strip on transverse stainless steel anchors forming an H-shape.

In the south lane (reduced pavement thickness over RAP base) the strain gauges were placed at the bottom of the AC layer, right on top of the RAP base layer. This corresponds to about 130 mm (5 inches) below the surface of the pavement. In the north lane (full thickness pavement on subgrade) the strain gauges were placed

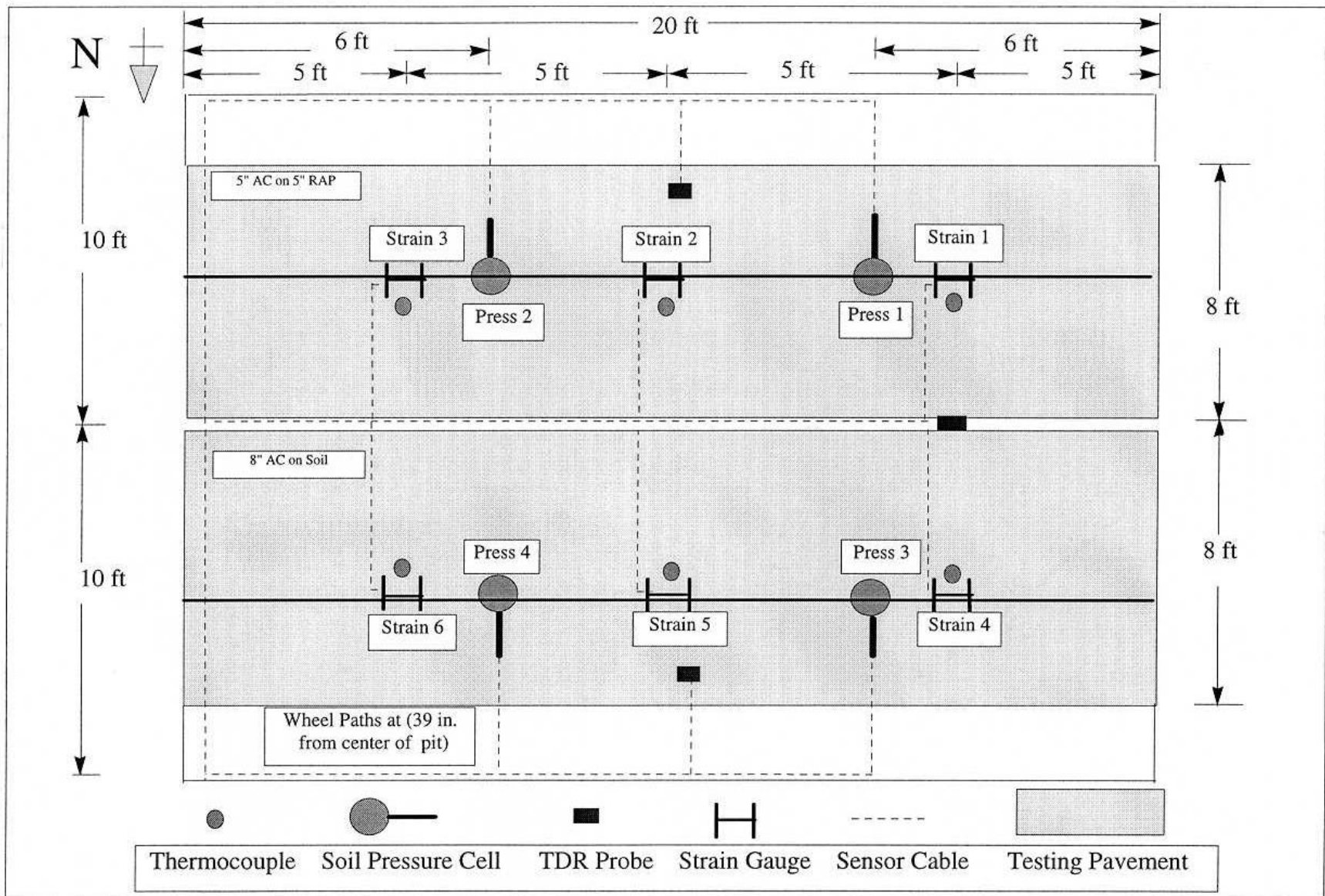


Figure 4.1 Location of Sensors in Nebraska Test (ATL-98-1)

below the AC layer, right on top of the subgrade soil, i.e., about 203 mm (8 in.) below the surface of the pavement.

The installation and hookup procedures followed the directions given by the manufacturer and the recommendations delineated by the Minnesota MnRoad Research project (Van Deusen *et al.*, 1992, and Baker *et al.*, 1994). Due to manufacturing complexity, the resistance of these strain gauges is not constant, but rather vary from one gauge to the other between 120 and 127 Ohms. For this reason, commercial ready-to-use strain indicators could not be used for signal conditioning. Special provisions had to be made for electric circuit bridge completion and signal amplification.

The gauges were intended for horizontal, longitudinal tensile strain measurements under the wheel passage. Strain traces similar to those reported by other experimental researchers (Heck *et al.*, 1998, for e.g.) were successfully obtained.

#### 4.4.1.2 Thermocouples

One thermocouple was placed next to each of the six strain gauges. These sensors read the temperature in the neighborhood of the strain gages below the pavement layer. They were intended for possible usage if temperature compensation would be necessary. Even though the strain gauges are supposed to have a self temperature compensation feature, it was thought that these thermocouples would be handy in case of abnormal instability or unexpected malfunction that might be attributed to excessive temperature sensitivity.

All six thermocouples were read and recorded daily to ensure that the temperatures below the pavement were mainly constant before starting the tests and relatively stable during the wheel load applications.

#### 4.4.1.3 Soil Pressure Cells

Four soil pressure cells, Model 3500 Dynamic Series with Ashcroft K1 Transducers (from Geokon), were placed as indicated in Figure 4.1 along the centerline of the wheel paths. This line is the same line along which the strain gauges were placed. Two pressure cells were therefore placed on each wheel path, at about 1.83 m (6 ft) from the east and west ends.

In the south lane (reduced pavement thickness over RAP base) the pressure cells were placed on the soil, below the RAP base layer. This corresponds to about 260 mm (10 in.) below the surface of the pavement. In the north lane (full thickness pavement on subgrade) the pressure cells were placed deeper in the subgrade soil, about 150 mm (6 in.) below the bottom of AC layer soil, i.e. about 350 mm (14 in.) below the surface of the pavement.

The pressure cells are constructed from two circular flat plates of 229 mm (9 in.)-

diameter welded together around their periphery. The plates are separated by a thin film of liquid which is connected through a tube to the pressure transducer. The transducer is connected to the data acquisition system by a conductor cable that is sealed into the transducer housing. It utilizes a bonded foil resistance strain gaged diaphragm that converts changes in pressure in a hydraulic flat-jack into a usable electrical signal.

The pressure cells were installed according to the manufacturer's guidelines and following the procedures recommended by the MnRoad research program. Pressure response traces similar to those reported by other experimental researchers (Ullidtz and Ekdahl, 1998, for e.g.) were obtained.

#### 4.4.1.4 Moisture Sensors

These are Time Domain Reflectometry (TDR) waveguide sensors installed in the subgrade. They are of the three-rod type acquired from SoilMoisture Equipment, Corp. The original TDR probes installed in the soil for the previous experiments were destroyed during removal of the pavement sections and the subbase. New probes were placed at more convenient locations as shown in Figure 4.1. Details about the installation procedure can be found in Melhem *et al.*, 1997 (Section 3.4.2, p 31). Moisture measurements were made with a TDR graphical cable tester (Tektronix Model 1502).

#### 4.4.2 Monitoring Plan

The monitoring/testing plan is shown in Table 4.1. The fourth column entitled "sensor data" indicates the frequency at which the strain and pressure sensors were recorded. Sensor data, transverse profiles, longitudinal profiles, nuclear density, and temperature readings were taken throughout the duration of the test. As shown in the second and third columns of the table, reduced loads were cautiously applied at first because the asphalt concrete mix was found to be somewhat soft after placement. In fact, it was originally planned to use a 97.8 kN (22,000 lb) single axle (overload) to accelerate failure, but because of the volumetric properties of the mix it was decided to use a standard axle to avoid excessive premature plastic deformation.

At the start, a 35.6 kN (8,000 lb) axle was used and conditions were closely monitored up to 5,000 load repetitions. Readings were taken every 1,000 repetitions. Then the axle load was increased to 80.1 kN (18,000 lb) and readings were taken every 2,500 repetitions up to 15,000 repetitions. At that time, the rate of rutting had decreased significantly and the volumetric changes had stabilized greatly. The load applications continued with the 80.1 kN (18,000 lb) standard axle and readings were taken regularly every 5,000 repetitions up to 65,000 repetitions and then at 67,000 repetitions.

Table 4.1 Monitoring Plan for ATL-98-1 Experiment

| Date    | Axle (kip) | No. of Reprs. | Sensor Data | Visual Inspection | Transverse Profile | Longitudinal Profile | Nuclear Density | Temp |
|---------|------------|---------------|-------------|-------------------|--------------------|----------------------|-----------------|------|
| 7/1/98  | 8          | 0             | X           | X                 | X                  | X                    | X               | X    |
| 8/3/98  | 8          | 1,000         | X           | X                 | X                  |                      |                 | X    |
| 8/4/98  | 8          | 2,000         | X           | X                 | X                  |                      |                 | X    |
| 8/5/98  | 8          | 3,000         | X           | X                 | X                  |                      |                 | X    |
| 8/6/98  | 8          | 4,000         | X           | X                 | X                  |                      |                 | X    |
| 8/7/98  | 8          | 5,000         | X           | X                 | X                  |                      |                 | X    |
| 8/10/98 | 18         | 7,500         | X           | X                 | X                  |                      |                 | X    |
| 8/11/98 | 18         | 10,000        | X           | X                 | X                  |                      | X               | X    |
| 8/12/98 | 18         | 12,500        | X           | X                 | X                  |                      |                 | X    |
| 8/13/98 | 18         | 15,000        | X           | X                 | X                  |                      |                 | X    |
| 8/14/98 | 18         | 20,000        | X           | X                 | X                  |                      | X               | X    |
| 8/17/98 | 18         | 25,000        | X           | X                 | X                  | X                    |                 | X    |
| 8/18/98 | 18         | 30,000        | X           | X                 | X                  |                      | X               | X    |
| 8/19/98 | 18         | 35,000        | X           | X                 | X                  |                      |                 | X    |
| 8/20/98 | 18         | 40,000        | X           | X                 | X                  |                      | X               | X    |
| 8/24/98 | 18         | 45,000        | X           | X                 | X                  |                      |                 | X    |
| 8/25/98 | 18         | 50,000        | X           | X                 | X                  | X                    | X               | X    |
| 8/26/98 | 18         | 55,000        | X           | X                 | X                  |                      |                 | X    |
| 8/27/98 | 18         | 60,000        | X           | X                 | X                  |                      |                 | X    |
| 8/28/98 | 18         | 65,000        | X           | X                 | X                  |                      | X               | X    |
| 8/31/98 | 18         | 67,000        | X           | X                 | X                  | X                    |                 | X    |

#### 4.5 Pavement Performance

The results of the instrumentation and experimental monitoring procedures are given in Appendix B. They are summarized below in the following sections.

##### 4.5.1 Horizontal Tensile Strains

Longitudinal tensile strain measurements were electronically taken using the strain gauges placed right below the AC pavement slabs. Strain traces due to the passage of the truck single axle were digitally recorded. These traces could also be seen on the computer screen as signals from the gauges were transmitted to the data acquisition system.

As indicated in the monitoring plan shown in Table 4.1, these measurements were made every working day towards the end of the application at the specified number of load repetitions while the wheel axle was kept rolling. After the data acquisition system had warmed up, strain signals would stabilize, noises would be eliminated, and displayed strain traces from all six gauges would appear more regular and more consistent. At this time two complete cycles are recorded consecutively for each gauge, one gauge at a time. Recording starts with a first cycle when the wheel carriage is heading from east to west (west bound #1). This is followed by the reversed rolling direction of this cycle (east bound #1). This is immediately followed by the two directions of the second recorded cycle (west bound #2, and east bound #2).

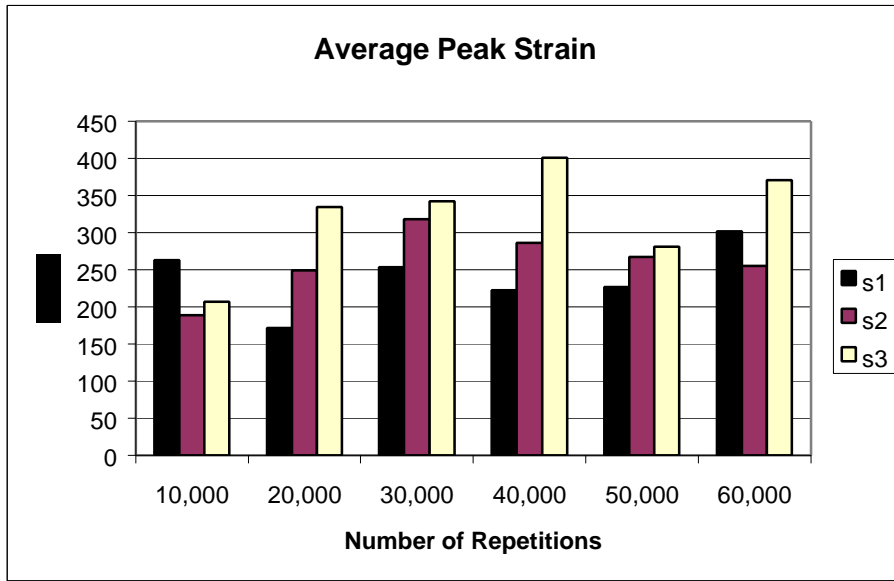
This procedure and sequence was used at all times for all recorded strain and pressure sensor data. A typical trace of two such cycles (four load repetitions) is shown in Figure B-1 of Appendix B for Strain Gage #1 during the first day of testing, after applying about 1,000 load repetitions. The complete trace of these four repetitions is shown in Figure B-2. Figure B-3 shows the comparison between the traces recorded after 7,500 load repetitions and those recorded after 25,000 repetitions.

The recorded peaks for each set of cycle pairs (four values) were averaged at increments of 10,000 load repetitions. Referring to Figure 4.1, each of the south and north lanes has three strain gauges designated s1, s2, s3, and s4, s5, s6, respectively. These are displayed in Figure 4.2 for (a) the reduced AC pavement on RAP (south lane), and (b) the full thickness AC pavement on subgrade (north lane).

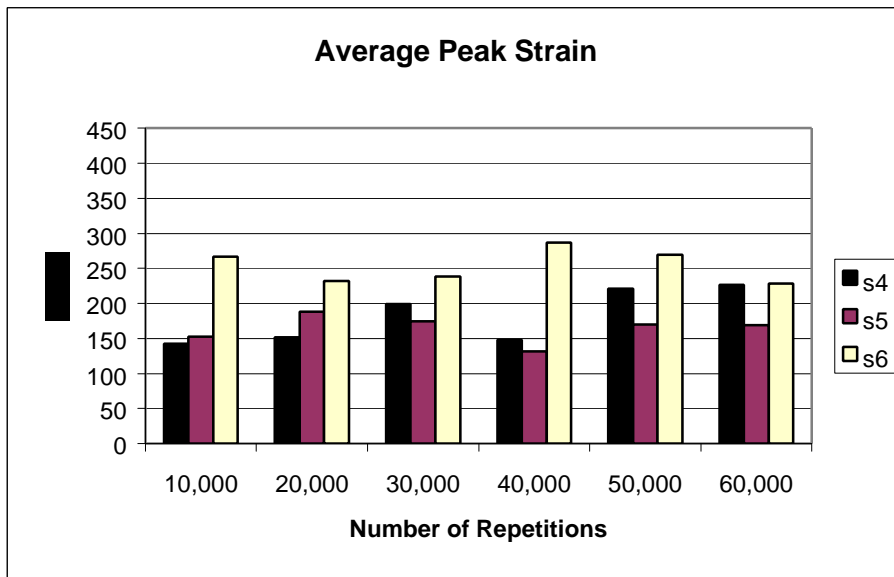
#### **4.5.2 Pavement Temperature**

Temperatures were recorded daily towards the end of the application of the specified number of load repetitions, at the time strains were to be recorded. Recorded values are shown in Figure B-4. It can be noted that while surface temperature was usually around 32°C (90°F), temperatures below the slabs were between 26 and 31°C (79 and 88°F).

The tabulated values indicate that during the first few days of the experiment, the temperature below the asphalt concrete pavement went only as high as 27°C (80°F). For the later part of the experiment, temperature values reached 31°C



(a) AC Pavement on RAP



(b) AC Pavement on Soil

**Figure 4.2 Variation of Peak Strains with Number of Load Repetitions**

(88°F). This is attributed to the fact that in the first few days, the number of repetitions applied was 1,000 or 2,500 which are reached in about 1:40 hrs and 4:10 hrs, respectively. However, when the number of load applications became 5,000 the testing machine, and consequently the radiant heaters, were kept running for about 8:20 hrs. During this longer time period, more heat was transmitted from the surface to the bottom of the pavement.

#### **4.5.3 Vertical Soil Pressure**

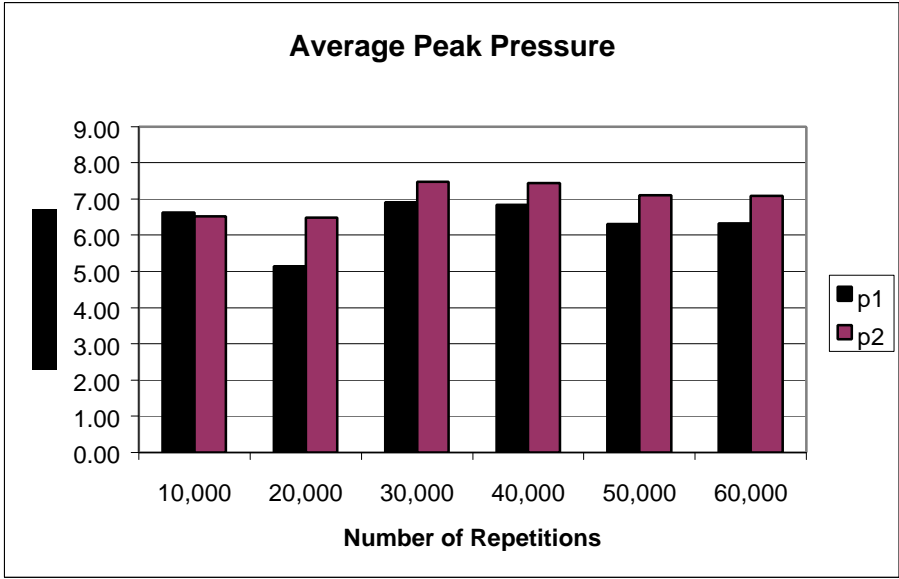
As in the case of strain gauges, soil pressure traces were digitally recorded under the passage of the truck axle. These traces were displayed on the computer screen as signals from the cells were transmitted to the data acquisition system. Signals from all four pressure cells were much more stable (with significantly less noise) than those from the strain gauges.

These measurements were made at about the same time as the strain measurements. As described in Section 4.5.1, two complete cycles were recorded consecutively for each pressure cell, one cell at a time. (Recording started for the first cycle when the wheel carriage is heading from east to west). A typical trace of such two cycles (four load repetitions) is shown in Figure B-5 of Appendix B for Pressure Sensor #1 after 1,000 load repetitions have been applied. As seen from the plots, the signals were very similar in shape and very close in magnitude. The numerical average for these four repetitions is plotted in Figure B-6. Figure B-7 shows the comparison between the traces recorded after 7,500 load repetitions and those recorded after 25,000 repetitions. The difference between the two does not seem to be very substantial. However, as seen in Figure B-8, the difference between the magnitude of the pressures at 1,000 and 25,000 is significant.

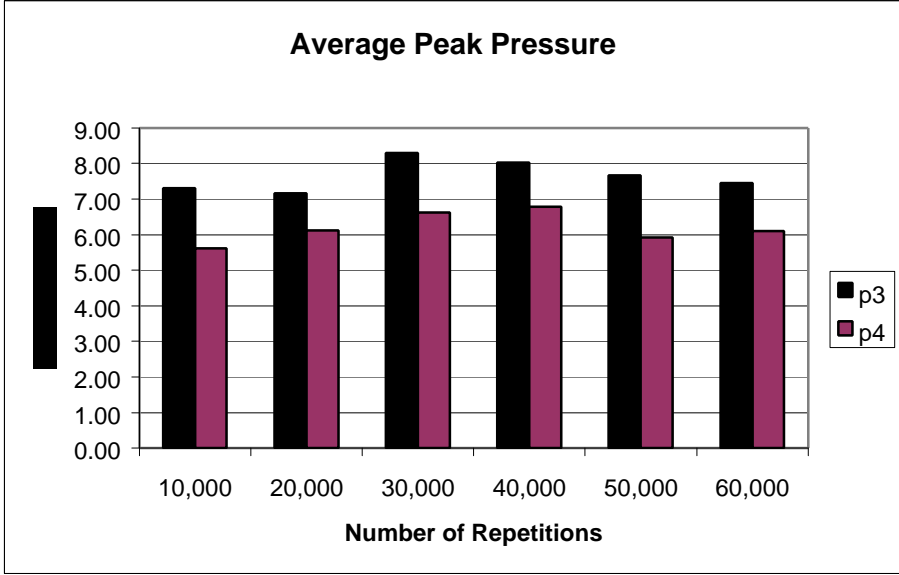
The peaks for each of the four recorded repetitions were averaged at increments of 10,000 load repetitions. Referring to Figure 4.1, each of the south and north lanes has two pressure cells designated p1, p2, and p3, p4, respectively. These are depicted in Figure 4.3 for (a) the reduced AC pavement on RAP (south lane), and (b) the full thickness AC pavement on subgrade (north lane).

#### **4.5.4 Asphalt Concrete Density**

The (wet) density of the asphalt concrete was measured at the beginning of the test, every 10,000 repetitions thereafter up to 50,000, and then at 65,000. The measurements were made at three locations on each of the north and south slabs, designated 1,2,3 and 4,5,6, respectively. These locations were selected at the quarter-span points along the north track of each pair of wheel paths. They correspond longitudinally to the location of the strain gauges embedded under the pavement.



(a) AC Pavement on RAP



(b) AC Pavement on Soil

Figure 4.3 Variation of Peak Pressure with Number of Load Repetitions

At each location, three one-minute readings of the nuclear gauge were taken and averaged. The variation of the asphalt concrete density with the number of load repetitions applied to the pavement sections is depicted in Figure 4.4. It can be observed that the values do not change significantly except from the initial conditions before any load is applied.

#### **4.5.5 Pavement Surface Rutting**

Surface rutting was measured using a Face Dipstick device. Surface elevations of the pavement are measured at 305 mm (12 in.)-intervals, corresponding to the swiveling feet of the apparatus. Readings were recorded manually as the device was moved along a straight path. A two-way passage on any given path allows corrections to be made such that the elevation of the ending point would correspond to that of the initial point and ensure that the loop is closed correctly. The change in elevation between the different loading stages indicates the progression of rutting, and comparison with the initial profile gives an indication of the total rut depth.

##### *4.5.5.1 Transverse Profiles*

As indicated in Table 4.1, transverse profiles were constructed at the beginning and at the end of the test, and at every intermediate loading step. The first few profiles were measured to keep track of the early rut, in case excessive premature plastic deformation would take place and the experiment would have to be stopped earlier than anticipated. Transverse profiles were measured along a line covering the width of both 2.44 m (8 ft)-slabs, for a total of 4.88 m (16 ft), starting always at the south edge of the south lane, going across to the north edge of the north lane, and back to the starting point. Transverse profiles followed chalk-lines traced at mid-span of the slabs (labeled “Middle Profiles”) and 1.52 m (5 ft) from the east and west ends (labeled “East Profiles” and “West Profiles, respectively”).

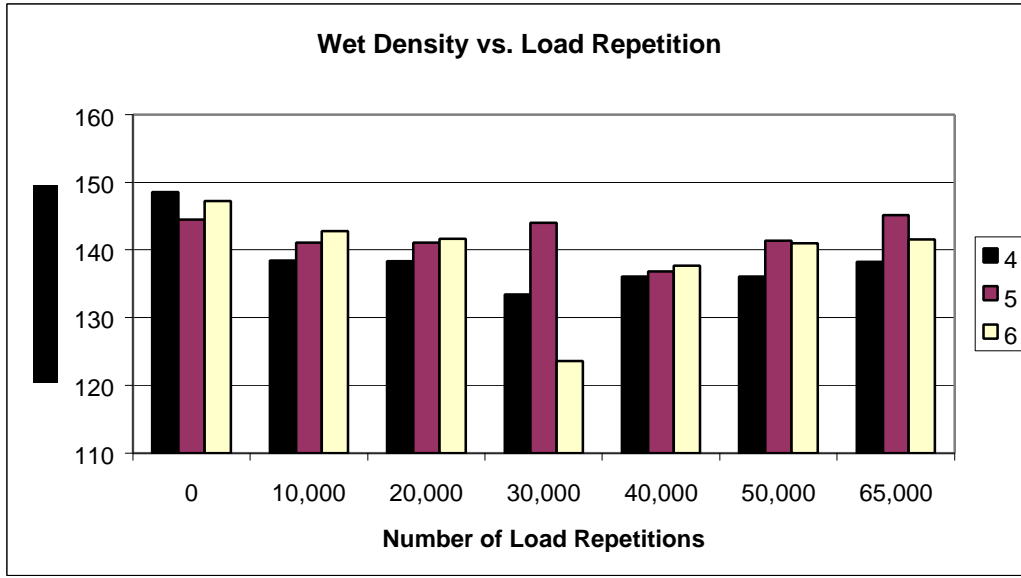
The progression of rutting is shown in Appendix B on Figures B-9, B-10, and B-11, for the East, Middle, and West profiles, respectively. The initial point was marked in the pavement so that the starting position would be the same every time a profile was to be taken.

The 305 mm (12 in.)-interval did not give enough accuracy to catch the peaks and valleys of all wheel tracks. For instance, the north lanes had always one point measured within each of its two wheel tracks. However, for the south lane, only one wheel track was caught in the East and West profiles and none in the Middle profiles. Note that even though the starting location was always the same every time for each transverse profile, the locations for the east, middle, and west starting points did not line up. Moreover, the 305 mm (12 in.)-intervals would miss the highest points (peaks) between the pair of wheel tracks.

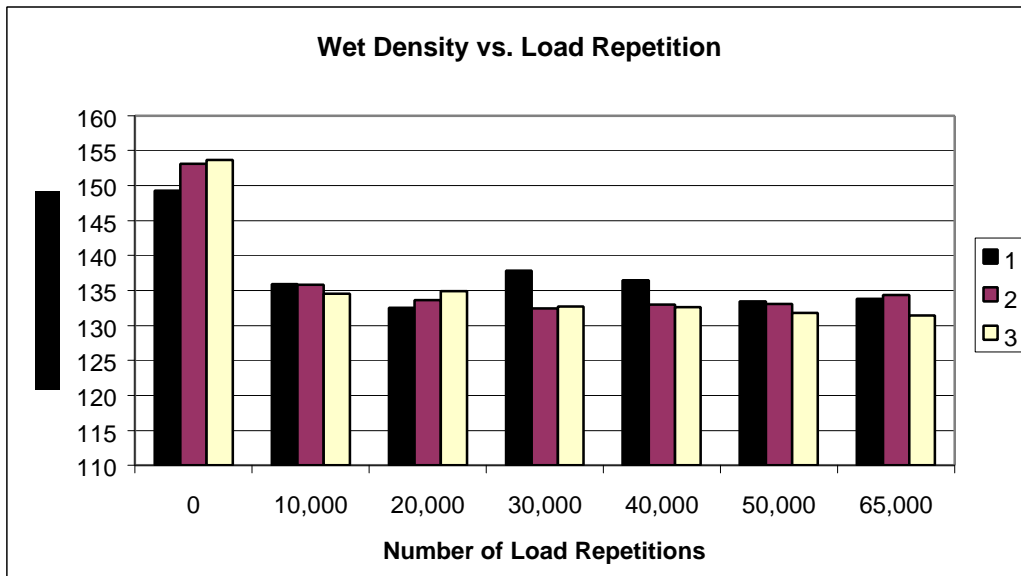
In general, the plots give a good idea about the degree of rutting in the slabs. In subsequent test, a more precise measuring device was implemented to give a better representation of the deflected shape of the wheel ruts, especially when used in combination with the longitudinal profiles.

|       |      |   |       |
|-------|------|---|-------|
|       | West |   |       |
|       | 4    | 1 |       |
| South | 5    | 2 | North |
|       | 6    | 3 |       |
|       | East |   |       |

**Nuclear Density Measurements**



(a) AC Pavement on RAP



(b) AC Pavement on Soil

Figure 4.4 Variation of Asphalt Concrete Density with Number of Load Repetitions

#### *4.5.5.2 Longitudinal Profiles*

Longitudinal profiles were also constructed using readings from the Face Dipstick device. These were measured along a line spanning the entire length of the slabs (6.1 m or 20 ft). Measurements started always at the east, going across to the north edge of the north lane, and back to the starting point. Longitudinal profiles followed chalk-lines traced at the center of the north track of the dual paths on both the AC pavement on soil and the AC on RAP (labeled “North Slab” and “South Slabs,” respectively).

The progression of rutting is shown in Appendix B on Figures B-12, and B-13 for the North and South slabs, respectively. It can be seen from these plots that the East portion of both slabs (represented by the first half of the profiles) had a dip at a distance of 1.52 m (5 ft) from the east point even before starting the test. This is reflected in the East transverse profiles (Figure B-9) that show deeper ruts than the Middle and West profiles (Figures B-10 and B-11).

#### *4.5.5.3 Cores*

A number of cores were drilled in the wheel path and away from the wheel path at the end of the experiment. These are indicated in Figure 4.5. The diameters of the cores were 102 mm (4 inches) and were drilled through the full depth of the pavement. The cores were taken by KDOT personnel and were sent to the Nebraska DOR for further analysis.

The visual inspection of the cores show a reduction in the thickness of the asphalt concrete layer between the core taken off the wheel paths and those taken from the wheel paths. These correspond to the degree of rutting observed at the surface of the pavement. This was an indication that the rutting was due to the plastic flow of the AC on the surface of the pavement under the wheel passage rather than compaction or settlement of the soil/RAP base beneath the pavement.

### **4.6 Conclusions**

The measurements of rutting, strain, stresses, and densities suggested that most of the changes in the pavement response occur in the first 5,000 to 10,000 load repetitions. When the asphalt mixes are new and relatively soft, much of the deformation and consequently strains take place at a high rate of change. After the first few thousand repetitions are applied, these changes occur at a much slower rate, and on the long-range, the performance of the two slabs tested in this experiment became very similar.

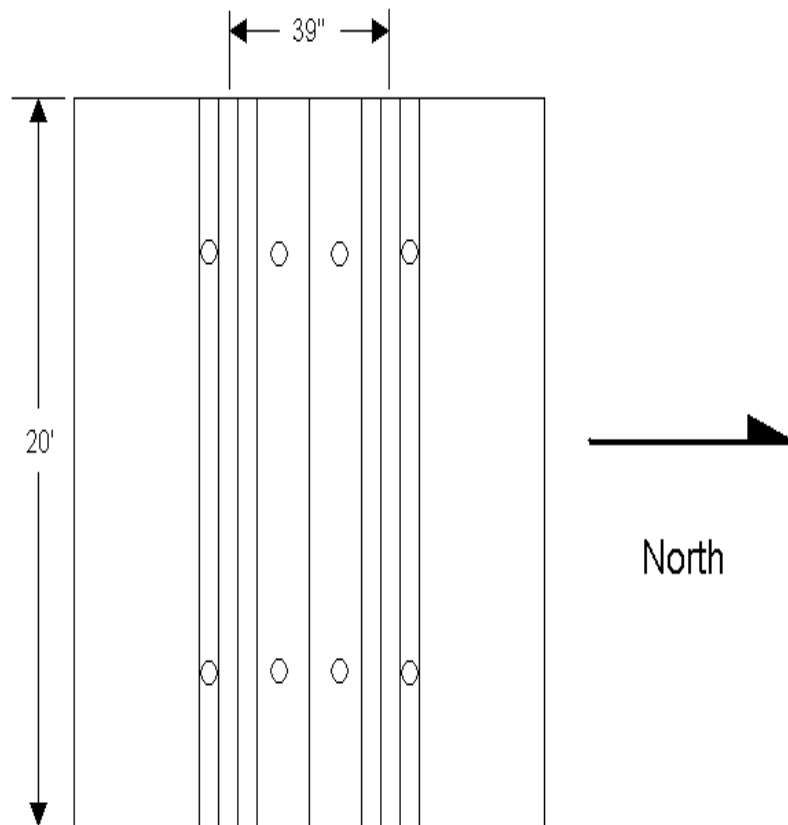


Figure 4.5 Location of Drilled Cores

The results observed from this experiment indicate that the performance of 127 mm (5 in.) of asphaltic concrete on 127 mm (5 in.) of asphaltic concrete millings with fine grained subgrade, when properly designed, was comparable and very close to that of a 203 mm (8 in.) layer of asphaltic concrete on fine grained silt-clay subgrade. In terms of cost efficiency, it is obvious that the 127 mm (5 in.) asphalt concrete layer on RAP is much less expensive than a 203 mm (8 in.) layer on asphalt concrete on soil, but yet it works as good.

It can be also concluded that the option of using a reduced AC thickness on RAP rather than a full thickness of AC directly on soil is a very valid alternative. In both cases, no aggregate or granular subbase was necessary. Of course this conclusion is made with respect to rutting and deformation under normal temperature and axle load repetitions. This does not apply to low temperature cracking under freezing or freeze/thaw conditions that were not studied in this experimental investigation.

## **5.0 PERFORMANCE OF A TYPICAL PAVEMENT REHABILITATION**

This chapter describes the second experiment performed under the Fiscal Year 98 contract (ATL-98-2), which is the sixth experiment conducted at the facility (ATL-Exp#6). This experiment was funded by the Midwest Accelerated Pooled Fund study. This experiment can be considered a continuation of the previous experiment because it involves the rehabilitation of the sections tested in ATL-Exp#5, and the application of additional load cycles. The ATL-Exp#5 was described in the previous chapter.

The purpose of this experiment is to study the performance and effectiveness of the repair performed on the distressed sections previously tested. This experiment also compares the two different types of pavement sections after their life was extended through the rehabilitation action.

### **5.1 Pavement Structure**

The pavement structure consists of the two original 2.44 m (8 ft)-wide lanes loaded side-by-side with a single axle up to 67,000 repetitions. The description of these lanes is given in Section 4.1. The repair consisted of milling 50 mm (2 inches) off the surface of the pavement and replacing them with 50 mm (2 inches) of appropriate hot mix asphalt concrete. The soil subgrade is the same as that of the previous experiment (see Section 4.2).

### **5.2 Specimen Preparation**

The specimen preparation consisted mainly of performing the repair on the distressed pavement. The repair was done by the same local highway construction company that is also a regular asphalt contractor to KDOT. Milling was done to the whole pavement, i.e. the entire length and width of both sections. This is shown in Figure 5.1. Except for a narrow longitudinal strip between the two slabs, the surface of the pavement was milled to a depth of about 50 mm (2 inches.) The holes caused by the core drilling were filled with the hot mix used for the overlay.

The hot asphalt mix added was a common Marshall mix being used during the time of the repair in a Kansas highway construction job. It was a typical KDOT mix (BM-2C). Bulk samples were given to the representative on the Technical Committee for the Nebraska Department of Roads who was also present during the section repair performed by contractor. The overlay was tacked to the milled surface using typical binder to ensure that the new layer is adequately bonded to the existing pavement structure.



Figure 5.1 Specimen After Milling of Entire Pavement

### 5.3 Testing Conditions

The testing conditions are the same as those of the previous experiment (see Section 4.3). Half the axle (a pair of wheels) was running on one slab while the other half was on the other slab. As in the previous test, no heating was necessary for this experiment. The overlay appeared to be of adequate strength and hardness and therefore it was deemed appropriate to apply the full load of the standard axle (18,000 lbs) from the beginning of the experiment.

It is worth mentioning that the wheel tracks were set to match the original tracks from the ATL-98-1 experiment. The location of the wheel paths during the first experiment was matched exactly in this experiment. This was done to ensure that the repair tested is exactly along the previous load path and therefore is at the location of maximum distress. Any densification of the existing asphalt layer or compaction of the soil beneath the pavement will be continued by the wheel loads applied here so that this will be a relevant continuation of the previous test.

## **5.4 Experiment Monitoring**

The same types of instrumentation and recording were used to record the pavement behavior as in the ATL-98-1 experiment. In fact, all sensors and gauges were preserved and re-used. This includes the strain gauges, thermocouples, the soil pressure cells, and the moisture sensors. After the repair job was completed, all sensors were tested and were found to be working properly.

For the type, location, and installation of the different sensors, please refer to Section 4.4 of the previous chapter. In addition to measurements obtained from these sensors, nuclear density measurements and surface profiles were recorded at the beginning of the experiment and periodically at the end of every 20,000 repetitions afterwards.

The monitoring/testing plan is shown in Table 5.1. The fourth column entitled "sensor data" indicates the frequency at which the strain and pressure sensors were recorded. Sensor data, transverse profiles, longitudinal profiles, nuclear density, and temperature readings were taken throughout the duration of the test. It can be seen from the second and third columns of the table, that an overload was used after about 84,000 repetitions were applied.

It can be noted that loads were applied every day of the week including weekends. This was done to shorten the overall experiment time duration so that the preparations could be made for the following test before the end of the hot asphalt production season. (The following experiment involves testing Superpave mixes with various ratios of river sand in the mixture.) That needed to be done during the month of October. Additional weekend work shifts were necessary to keep up with this pace. However, all testing was done during the day when the temperature was fairly high most of the time (no night shifts were used).

## **5.5 Pavement Performance**

The results of the instrumentation and experimental monitoring procedures closely follow those of the ATL-98-1 experiment. They are summarized below in the following sections.

### **5.5.1 Horizontal Tensile Strains**

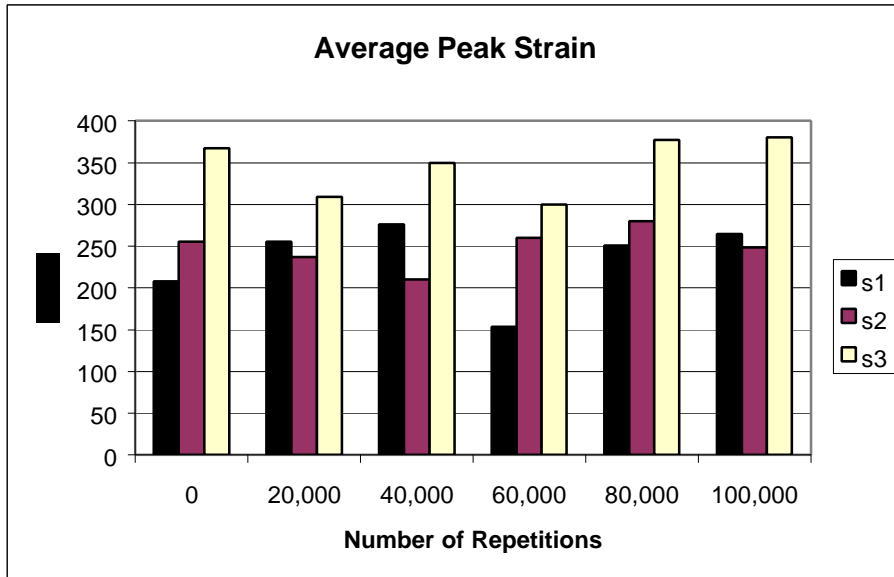
Longitudinal tensile strain measurements were electronically taken using the strain gauges placed right below the AC pavement slabs. Strain traces were digitally recorded due to the passage of the truck single axle. As indicated in the monitoring plan shown in Table 5.1, these measurements were made following the application of 20,000 load repetitions. The same procedures as before were followed so that the strain signals would stabilize, noises would be eliminated, and displayed strain traces from all six gauges would appear relatively regular and consistent. The procedure and sequence described in Section 4.5.1 were used at all times for all

recorded strain and pressure sensor data.

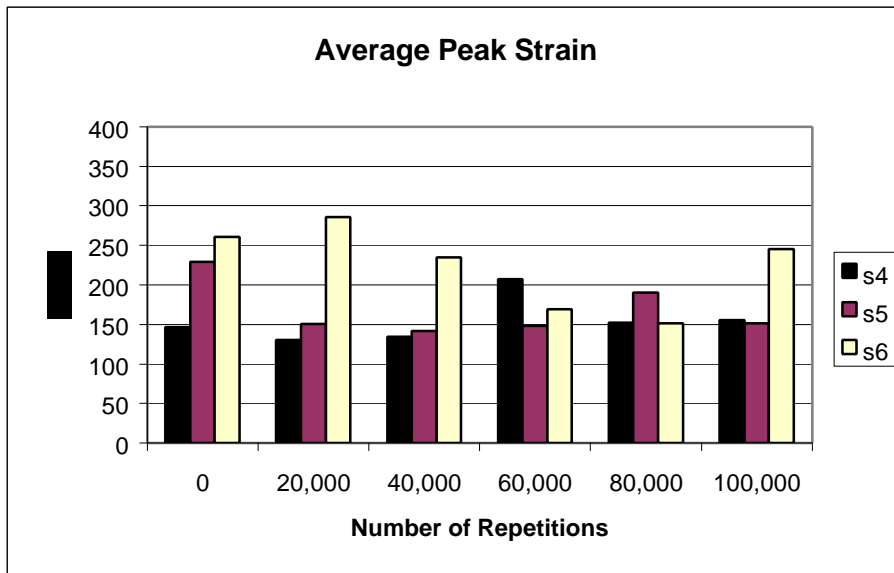
The recorded peaks for each set of cycle pairs (four values) were averaged at increments of 20,000 load repetitions. Referring to Figure 4.1, each of the south and north lanes has three strain gauges designated s1, s2, s3, and s4, s5, s6, respectively. These are displayed in Figure 5.2 for (a) the reduced AC pavement on RAP (south lane), and (b) the full thickness AC pavement on subgrade (north lane).

Table 5.1 Monitoring / Testing Plan for ATL-98-2 Experiment

| Date    | Axle (kip) | No of Reps. | Sensor Data | Visual Inspection | Transverse Profile | Longitudinal Profile | Nuclear Density | Temp |
|---------|------------|-------------|-------------|-------------------|--------------------|----------------------|-----------------|------|
| 9/10/98 | 18         | 416         | X           | X                 | X                  | X                    | X               | X    |
| 9/11/98 | 18         | 5,318       |             |                   |                    |                      |                 |      |
| 9/14/98 | 18         | 12,292      |             |                   |                    |                      |                 |      |
| 9/15/98 | 18         | 20,000      | X           | X                 | X                  | X                    | X               | X    |
| 9/15/98 | 18         | 20,400      |             |                   |                    |                      |                 |      |
| 9/16/98 | 18         | 29,380      |             |                   |                    |                      |                 |      |
| 9/17/98 | 18         | 38,348      |             |                   |                    |                      |                 |      |
| 9/18/98 | 18         | 40,000      | X           | X                 | X                  | X                    | X               | X    |
| 9/18/98 | 18         | 44,304      |             |                   |                    |                      |                 |      |
| 9/19/98 | 18         | 48,820      |             |                   |                    |                      |                 |      |
| 9/20/98 | 18         | 51,794      |             |                   |                    |                      |                 |      |
| 9/21/98 | 18         | 59,676      |             |                   |                    |                      |                 |      |
| 9/22/98 | 18         | 60,000      | X           | X                 | X                  | X                    | X               | X    |
| 9/22/98 | 18         | 66,692      |             |                   |                    |                      |                 |      |
| 9/23/98 | 18         | 75,080      |             |                   |                    |                      |                 |      |
| 9/24/98 | 18         | 80,000      | X           | X                 | X                  | X                    | X               | X    |
| 9/24/98 | 18         | 82,874      |             |                   |                    |                      |                 |      |
| 9/25/98 | 18         | 83,690      |             |                   |                    |                      |                 |      |
| 9/25/98 | 22         | 91,174      |             |                   |                    |                      |                 |      |
| 9/28/98 | 22         | 100,000     | X           | X                 | X                  | X                    | X               | X    |



(a) AC Pavement on RAP



(b) AC Pavement on Soil

Figure 5.2 Variation of Peak Strains with Number of Load Repetitions

### **5.5.2 Pavement Temperature**

Temperatures were recorded towards the end of the application of the specified number of load repetitions, at the time strains were to be recorded. Recorded values are shown in Figure 5.3. It can be noted that surface temperature was mostly below 32°C (90°F) because testing was done in September (as opposed to ATL-98-1 which was done in August). However on the average, temperatures below the slabs were between 25°C and 33°C (77°F and 83°F).

### **5.5.3 Vertical Soil Pressure**

As described in Section 4.5.1, two complete cycles were recorded consecutively for each pressure cell, one cell at a time. (Recording started for the first cycle when the wheel carriage was heading from east to west). The peaks for each of the four recorded repetitions were averaged at increments of 20,000 load repetitions. Referring to Figure 4.1, each of the south and north lanes have two pressure cells designated p1, p2, and p3, p4, respectively. The peaks from these cells are depicted in Figure 5.4 for (a) the reduced AC pavement on RAP (south lane), and (b) the full thickness AC pavement on subgrade (north lane).

### **5.5.4 Asphalt Concrete Density**

The (wet) density of the asphalt concrete was measured at the beginning of the test and every 20,000 repetitions until the end of the test. As before, measurements were made at three locations on each of the north and south slabs, designated 1,2,3 and 4,5,6, respectively. These locations correspond longitudinally to the location of the strain gauges embedded under the pavement.

At each location, three one-minute readings of the nuclear gauge were taken and averaged. The variation of the asphalt concrete density with the number of load repetition applied to the pavement sections is depicted in Figure 5.5. It can be observed that the values vary relatively more when compared to those in the previous test before the overlay.

| Date    | Sensor Location/ Designation |       |       |            |       |       |
|---------|------------------------------|-------|-------|------------|-------|-------|
|         | North Slab                   |       |       | South Slab |       |       |
|         | No. 4                        | No. 7 | No. 9 | No. 3      | No. 6 | No. 8 |
| 9/10/98 | 78.5                         | 78.5  | 78.9  | 79.3       | 78.9  | 79.8  |
| 9/15/98 | 82.1                         | 82.2  | 82.6  | 83.1       | 82.9  | 83.0  |
| 9/18/98 | 79.7                         | 79.5  | 79.7  | 79.6       | 79.5  | 79.9  |
| 9/22/98 | 77.8                         | 77.5  | 77.3  | 77.4       | 76.8  | 78.0  |
| 9/24/98 | 78.3                         | 77.4  | 78.3  | 79.2       | 78.1  | 79.2  |
| 9/29/98 | 80.9                         | 81.3  | 80.9  | 80.3       | 80.9  | 80.5  |

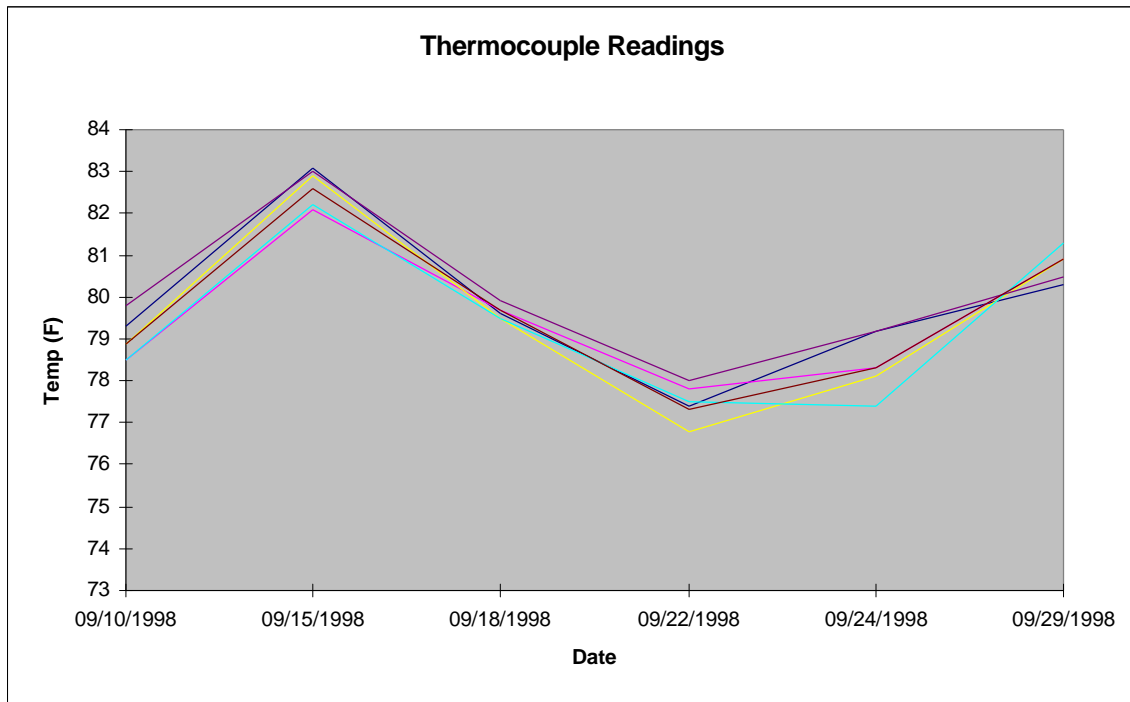
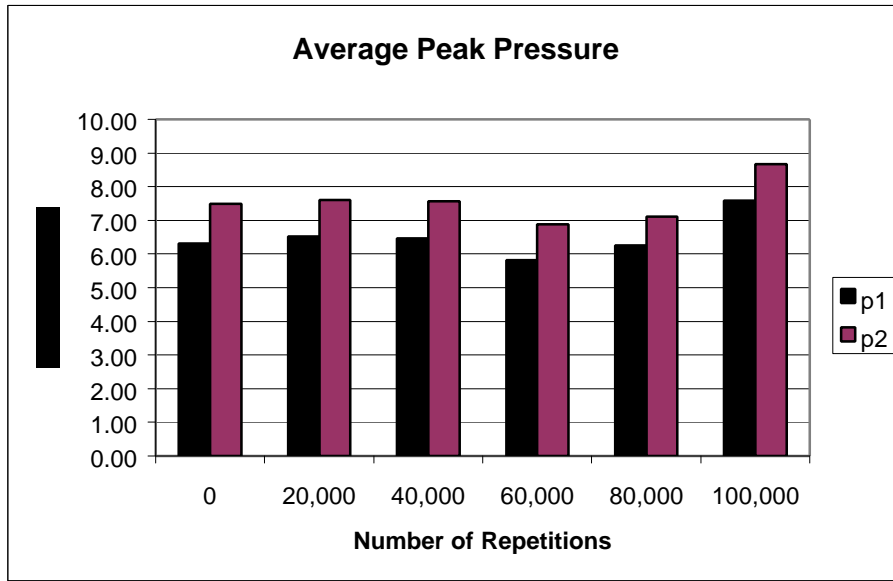
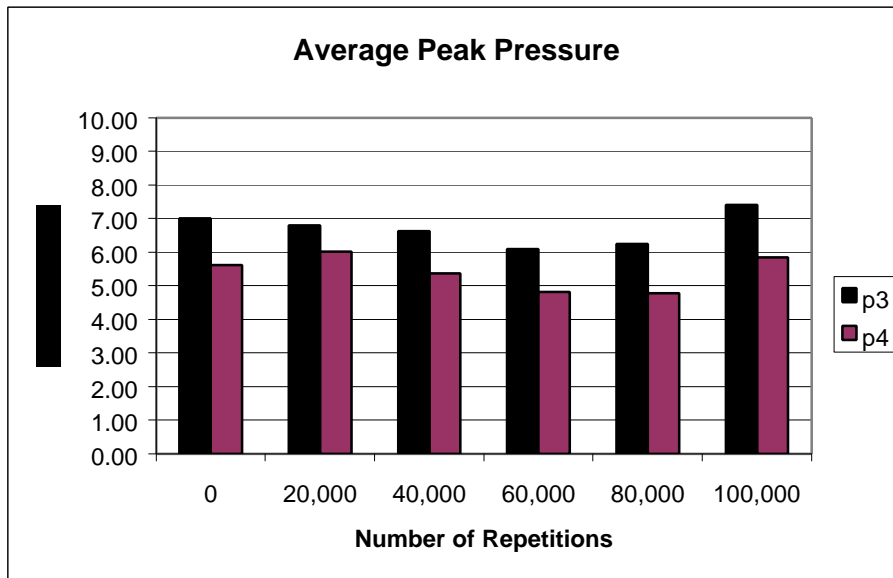


Figure 5.3 Thermocouple Readings for ATL-98-2 Experiment (0-100,000 Repetitions)



(a) AC Pavement on RAP

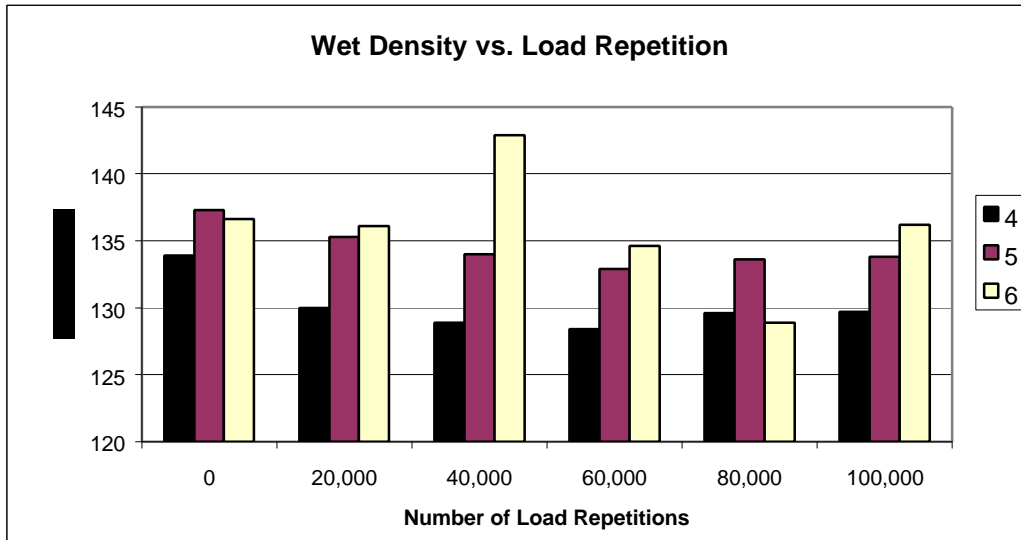


(b) AC Pavement on Soil

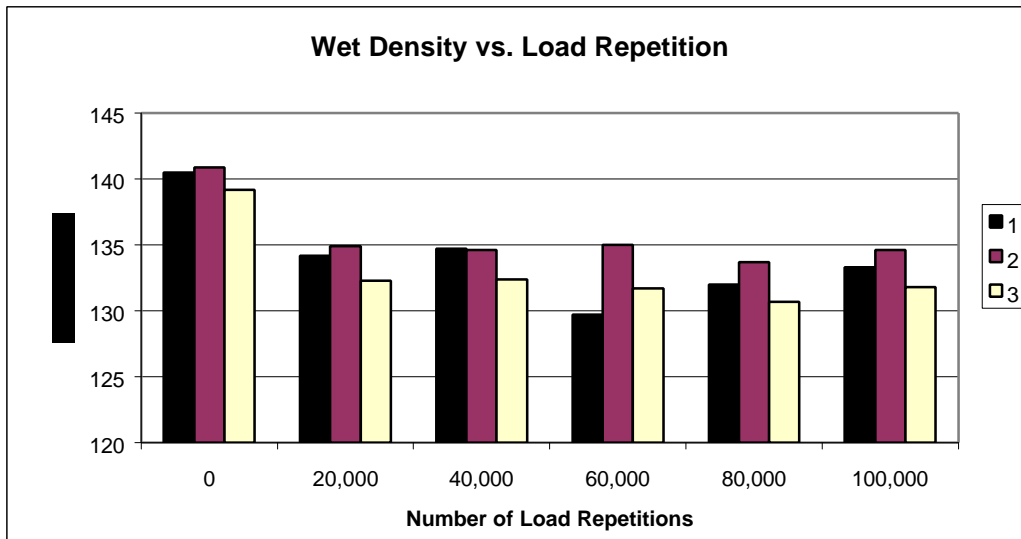
Figure 5.4 Variation of Peak Pressure with Number of Load Repetitions

|       |      |   |       |
|-------|------|---|-------|
|       | West |   |       |
|       | 4    | 1 |       |
| South | 5    | 2 | North |
|       | 6    | 3 |       |
|       | East |   |       |

**Nuclear Density Measurements**



(a) AC Pavement on RAP



(b) AC Pavement on Soil

Figure 5.5 Variation of Asphalt Concrete Density with Number of Load Repetitions

## **5.5.5 Pavement Surface Rutting**

### *5.5.5.1 Transverse Profiles*

As indicated in Table 5.1, transverse profiles were constructed at the beginning and at the end of the test, and at every intermediate loading step. Transverse profiles were measured along a line covering the width of both 2.44 m (8 ft)-slabs, for a total of 4.88 m (16 ft), starting always at the south edge of the south lane, going across to the north edge of the north lane, and back to the starting point. Transverse profiles followed chalk-lines traced at mid-span of the slabs (labeled "Middle Profiles") and 1.52 m (5 ft) from the east and west ends (labeled "East Profiles" and "West Profiles", respectively). The progression of rutting is shown in Appendix C on Figures C-1, C-2, and C-3, for the East, Middle, and West profiles, respectively. The initial point was marked in the pavement so that the starting position would be the same every time a profile was to be taken.

### *5.5.5.2 Longitudinal Profiles*

Longitudinal profiles were measured along a line spanning the entire length of the slabs (6.1 m or 20 ft). Measurements started always at the east, going across to the north edge of the north lane, and back to the starting point. Longitudinal profiles followed chalk-lines traced at the center of the north track of the dual paths on both the AC pavement on soil and the AC on RAP (labeled "North Slab" and "South Slabs," respectively). The progression of rutting is shown in Appendix C in Figures C-4 and C-5 for the North and South slabs, respectively.

## **5.6 Conclusions**

The results observed from this experiment indicate that milling and replacing the top 50 mm (2 inches) from the surface of 127 mm (5 in.) of asphaltic concrete on 127 mm (5 in.) of asphaltic concrete millings with fine grained subgrade, or from the surface of a 203 mm (8 in.) layer of asphaltic concrete on fine grained silt-clay subgrade is an adequate pavement repair procedure. The overlay resisted 84,000 repetitions of a standard 80.1 kN (18,000 lb) axle and an additional 16,000 repetitions of an overload axle of 97.9 kN (22,000 lbs).

Referring to the original structure of the pavement, it is obvious that the 127 mm (5 in.) asphalt concrete layer on RAP is quite comparable to a 203 mm (8 in.) layer on asphalt concrete on soil. Including the repair done at 67,000 repetitions both sections were subjected to a total of 167,000 load repetitions. Longitudinal strains, vertical soil pressure, material densities, and rutting were very close in both cases.

It should be noted that actual service life of similar pavements on the highway will be much longer than the one experienced in the accelerated testing environment. The frequency of occurrence of high axle-loads being applied exactly on the same path and at the rate of 10 repetitions per minute (600 repetitions per hour) is higher

than normal traffic conditions. Even on heavy traffic highways, chances are slim that the same type of load axles will hit the exact same spots on the wheel path so frequently. On the other hand, it has been established that the axle of a testing machine (such as that of the K-ATL moving at a speed of 5-7 mph) produces much more damage than those of trucks running at 60 or 70 mph. This is mainly due to the fact that the tires of the slower axles are in contact with the surface at any certain spot along the path much longer than tires of a running truck. These are all characteristics of accelerated pavement testing.

Accelerated pavement testing can give a very good performance assessment when two pavement mixes or pavement types are compared side-by-side. The relative behavior is a good qualitative indication of pavement performance. It gives a general evaluation of how well an alternate design works when compared to a typical design. In the current case, it can be concluded that the option of using a reduced AC thickness on RAP rather than a full thickness of AC directly on soil is a very valid alternative, even when no aggregate or granular subbase is used.

Data collected for longitudinal tensile strains below the pavement, soil pressure in the subgrade, asphalt wet densities, material testing, and surface elevations and profile curves have been collected, properly classified, and documented. Such data can be used in further research and more detailed analysis. It is made available to future analytical studies and is suitable for comparison with results from numerical modeling and computational methods.

**APPENDIX A**  
**MARSHALL MIX DESIGN DATA**

**MARSHALL MIXTURE DESIGN DATA**

Project location: ATL Test Section Nebraska Mix Design

Asphalt grade: AC 10

Temperature Mixing:292-302F

Compaction:272-282F

**Grading of Available Aggregates:**

| Sieve size<br>(mm) | %Retained                             |                         |                        |                     |
|--------------------|---------------------------------------|-------------------------|------------------------|---------------------|
|                    | Crushed<br>Limestone<br>(CS-1) (3/4") | Dolose (new)<br>3/8 in. | Sand Gravel<br>(SSG-1) | Screening<br>(CS-2) |
| #200               | 98                                    | 99.4                    | 99                     | 81                  |
| #100               | 98                                    | 99.3                    | 96                     | 77                  |
| #50                | 98                                    | 99.1                    | 84                     | 71                  |
| #30                | 98                                    | 98.8                    | 61                     | 64                  |
| #16                | 98                                    | 97.7                    | 38                     | 54                  |
| #8                 | 98                                    | 91.8                    | 18                     | 39                  |
| #4                 | 98                                    | 25.6                    | 5                      | 18                  |
| 3/8"               | 81.2                                  | 0                       | 0                      | 1                   |
| 1/2"               | 66                                    | 0                       | 0                      | 0                   |
| 3/4"               | 0                                     | 0                       | 0                      | 0                   |
| 1"                 | 0                                     | 0                       | 0                      | 0                   |

**Individual Aggregate Specific Gravities:**

| Aggregate | Bulk sp. gr. | % Crushed |
|-----------|--------------|-----------|
| CS-1      | 2.529        | 100       |
| Dol Shot  | 2.67         | 100       |
| SSG-1     | 2.599        | 0         |
| CS-2      | 2.51         | 100       |

**Design Aggregate Blend:**

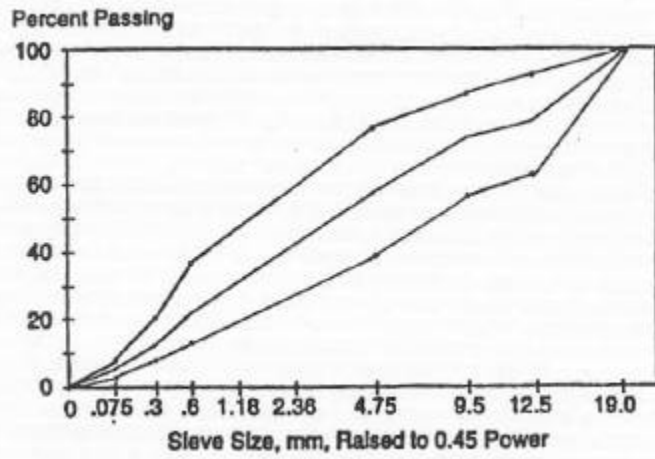
|         | CS-1 | Dolose | SSG-1 | CS-2 | % crushed |
|---------|------|--------|-------|------|-----------|
| Blend 1 | 0.3  | 0.15   | 0.35  | 0.2  | 65        |
| Blend 2 | 0.35 | 0.2    | 0.25  | 0.2  | 75        |
| Blend 3 | 0.3  | 0.3    | 0.2   | 0.2  | 80        |

**Gradation Curve Data:**

| Sieve size, n | % Retained |         |        | control poin<br>Min | TYPE 14<br>Mid Point | Max |
|---------------|------------|---------|--------|---------------------|----------------------|-----|
|               | Blend 1    | Blend 2 | Blend3 |                     |                      |     |
| 200           | 95.16      | 95.13   | 95.22  | 93                  | 95                   | 97  |
| 100           | 93.295     | 93.56   | 93.79  |                     |                      |     |
| 50            | 87.865     | 89.32   | 90.13  | 79                  | 86                   | 92  |
| 30            | 78.37      | 82.11   | 84.04  | 62                  | 74                   | 86  |
| 16            | 63.155     | 74.14   | 77.11  |                     |                      |     |

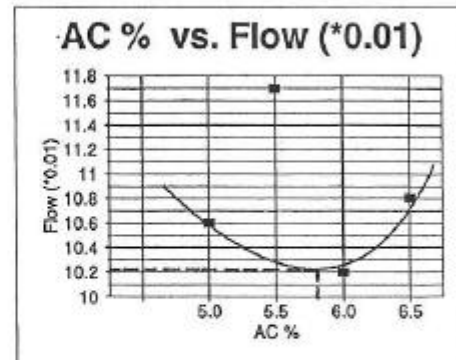
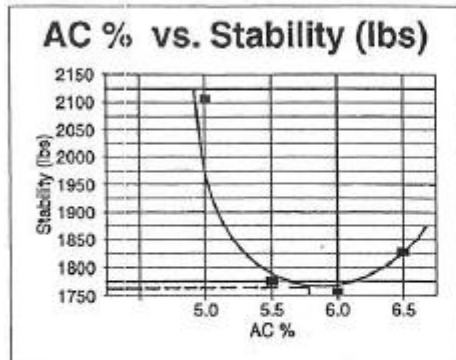
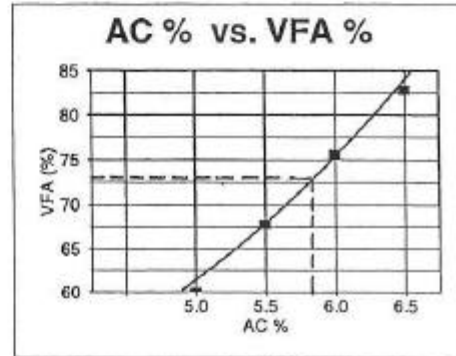
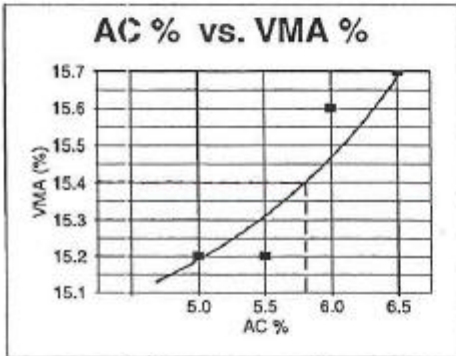
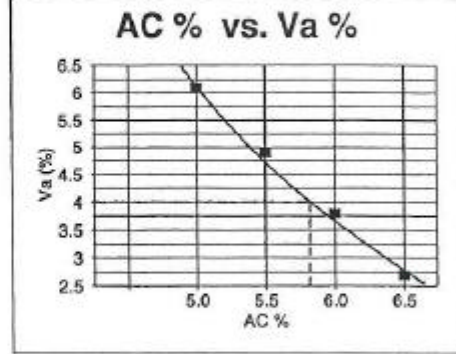
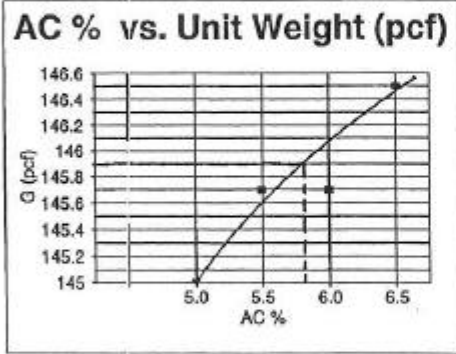
|      |       |       |       |    |    |    |
|------|-------|-------|-------|----|----|----|
| 8    | 57.27 | 64.96 | 68.34 |    |    |    |
| 4    | 38.59 | 44.27 | 41.68 | 22 | 40 | 58 |
| 3/8" | 24.56 | 28.62 | 24.56 | 12 | 26 | 40 |
| 1/2" | 19.8  | 23.1  | 19.8  | 7  | 16 | 24 |
| 3/4" | 0     | 0     | 0     | 0  | 1  | 2  |
| 1"   | 0     | 0     | 0     |    |    |    |

Blend 1 was selected as the design blend for the mix design.



**NEBRASKA MIX DESIGN**

| AC (%) | Unit Wt. (pcf) | Va (%) | VMA (%) | VFA (%) | Stability (lbs) | Flow |
|--------|----------------|--------|---------|---------|-----------------|------|
| 5.0    | 145.0          | 6.1    | 15.2    | 60.0    | 2106            | 10.6 |
| 5.5    | 145.7          | 4.9    | 15.2    | 67.8    | 1776            | 11.7 |
| 6.0    | 145.7          | 3.8    | 15.6    | 75.6    | 1756            | 10.2 |
| 6.5    | 146.5          | 2.7    | 15.7    | 82.8    | 1828            | 10.8 |



Design A.C. (%) = 5.8

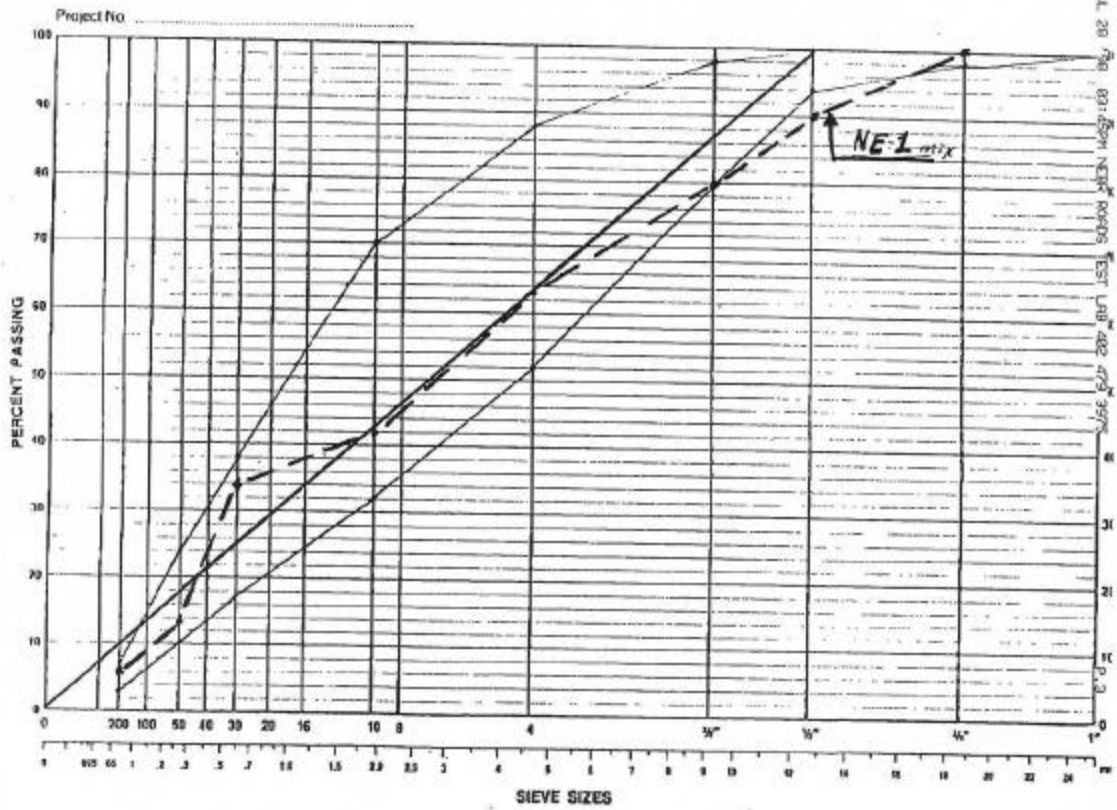
50 blow Marshall

| Parameter               | Design Value | Criteria |
|-------------------------|--------------|----------|
| Air Voids (%)           | 4            | 4        |
| VMA (%)                 | 15.4         | 15       |
| % Crushed Value         | 65           | 60       |
| Maximum Limestone       | 30           | 60       |
| VFA (%)                 | 74           |          |
| Marshall Stability (lb) | 1765         |          |
| Flow (1/100 in.)        | 10.2         |          |

# GRADATION CHART

SIEVE SIZES RAISED TO 0.45 POWER

*1/2" Band*



**APPENDIX B**

**TYPICAL RESULTS FROM ATL-98-1 EXPERIMENT**

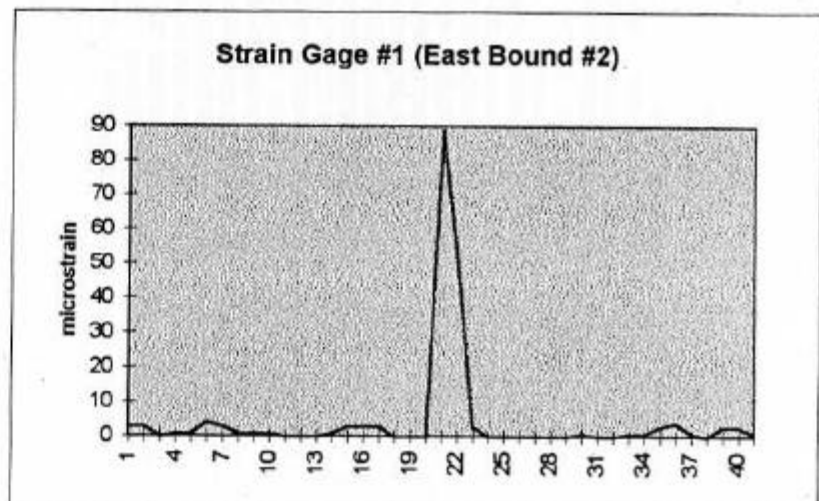
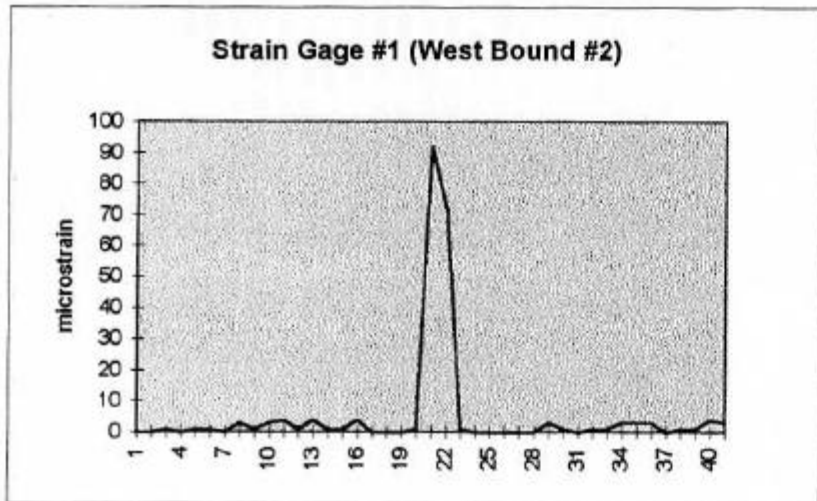
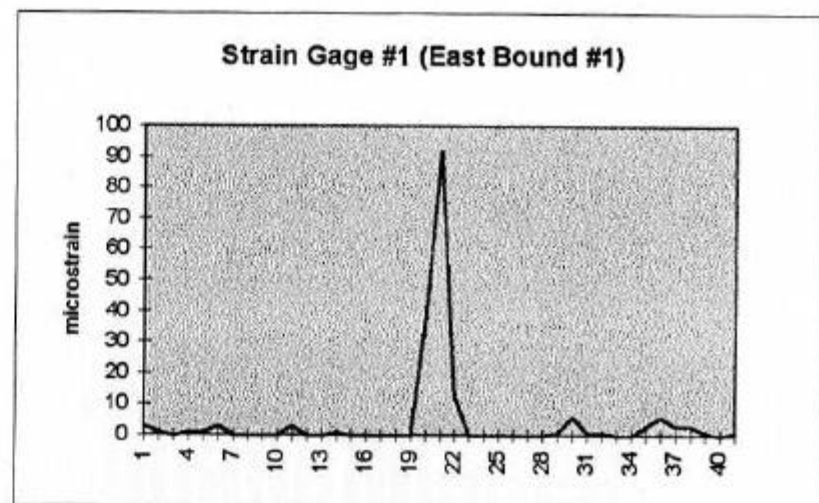
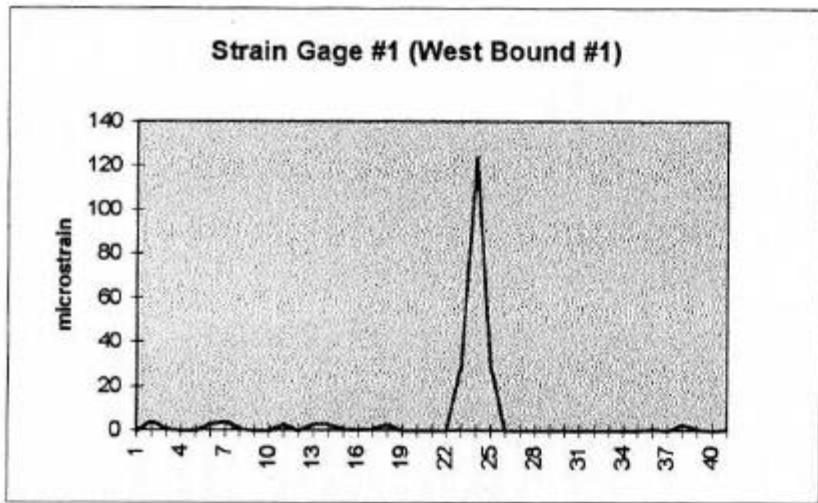


Figure B.1 Strain Gage Data at 1000 Load Repetitions for Strain Gage #1

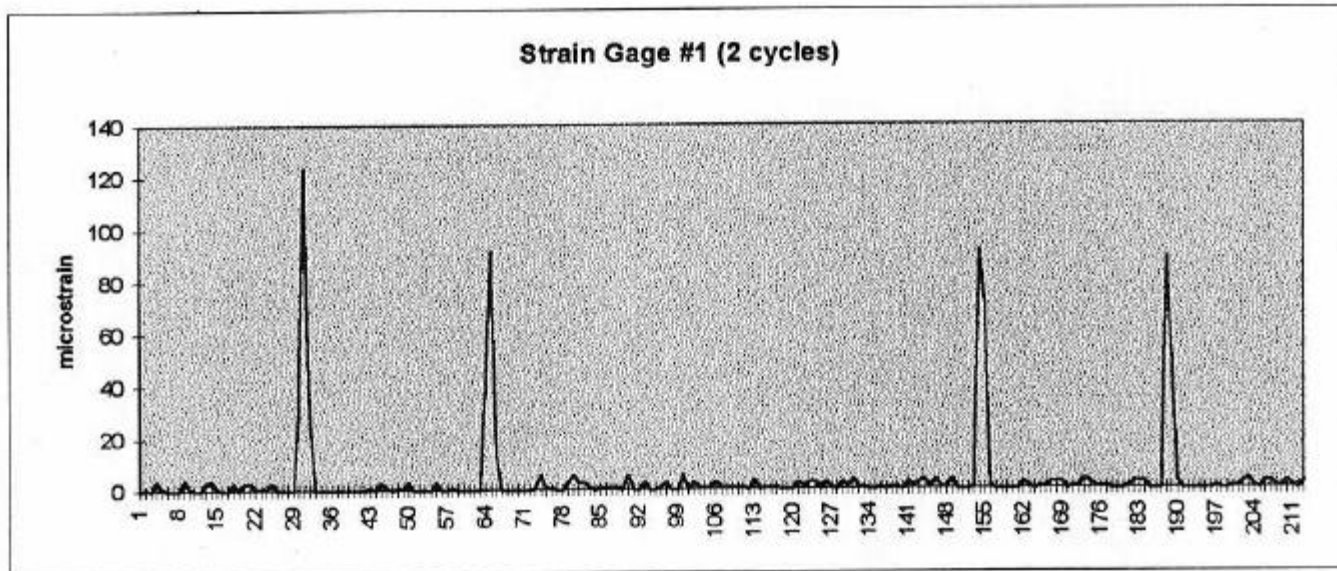


Figure B.2 Full Trace of Two Complete Cycles

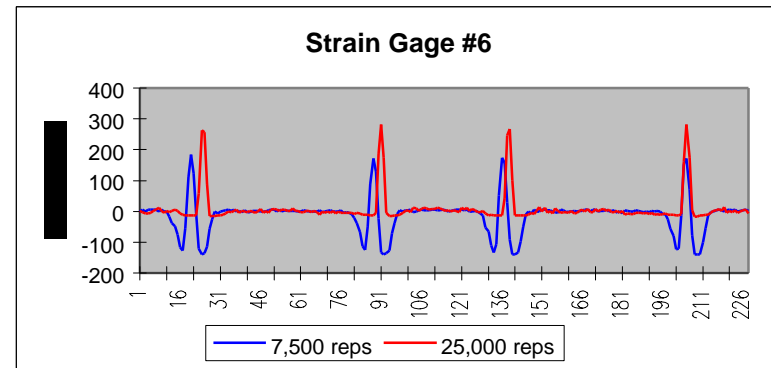
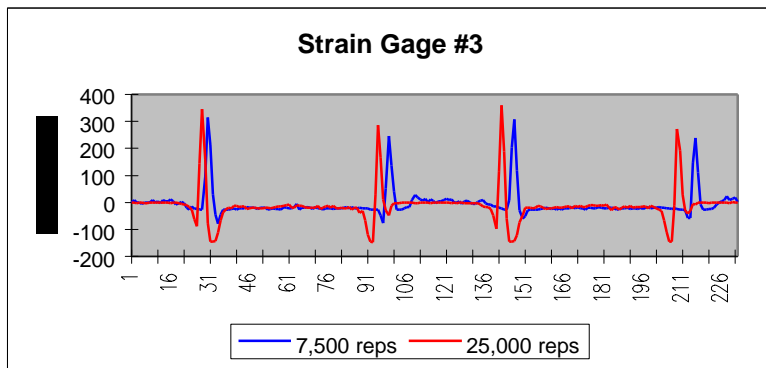
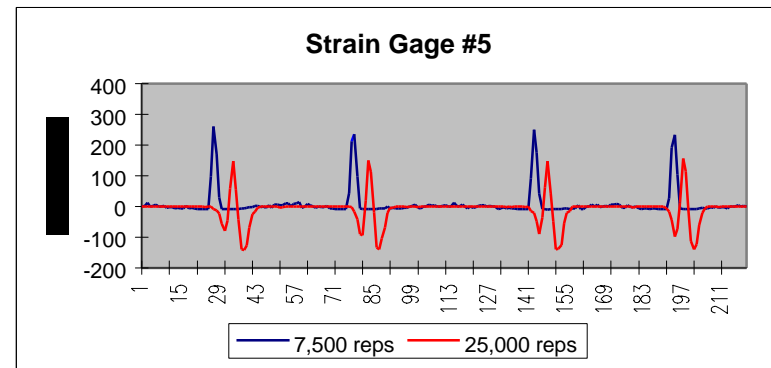
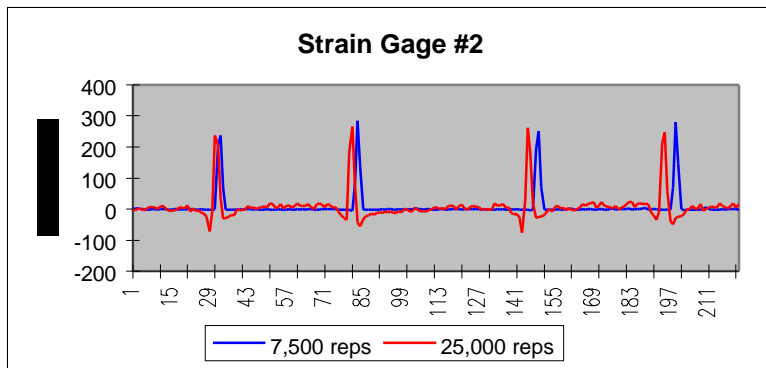
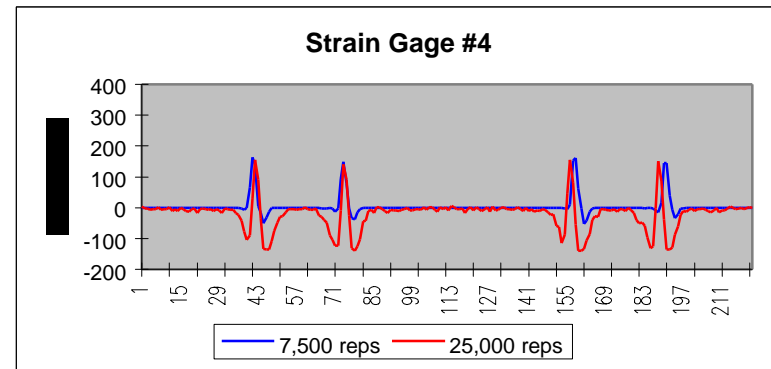
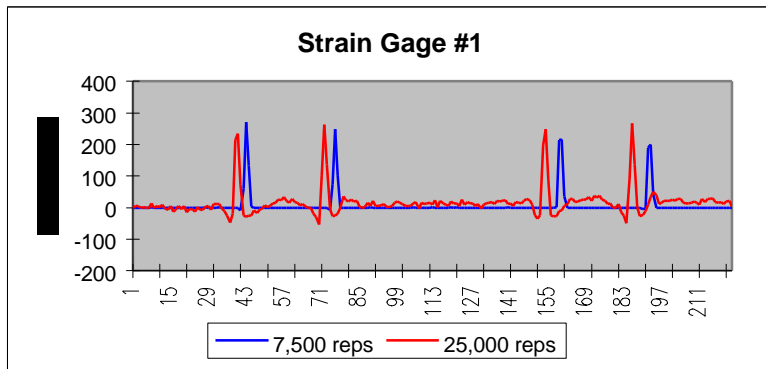


Figure B.3 Comparison of Strains Between 7,500 and 25,000 Repetitions  
(Load Repetition at 18 kips)

| Date    | Sensor Location/ Designation |       |       |            |       |       |
|---------|------------------------------|-------|-------|------------|-------|-------|
|         | North Slab                   |       |       | South Slab |       |       |
|         | No. 4                        | No. 7 | No. 9 | No. 3      | No. 6 | No. 8 |
| 8/4/98  | 79.8                         | 80.2  | 80.0  | 80.0       | 80.1  | 79.6  |
| 8/5/98  | 79.4                         | 79.4  | 79.1  | 79.1       | 79.6  | 79.3  |
| 8/6/98  | 79.3                         | 79.3  | 79.3  | 79.3       | 79.2  | 79.1  |
| 8/7/98  | 78.7                         | 78.2  | 78.1  | 78.3       | 78.4  | 78.1  |
| 8/10/98 | 79.7                         | 79.4  | 79.1  | 79.4       | 79.5  | 79.2  |
| 8/11/98 | 80.1                         | 80.6  | 80.7  | 80.8       | 80.9  | 81.0  |
| 8/12/98 | 79.0                         | 79.2  | 79.0  | 79.5       | 79.0  | 79.0  |
| 8/13/98 | 79.2                         | 79.0  | 79.5  | 79.1       | 79.4  | 79.7  |
| 8/14/98 | 79.9                         | 80.4  | 80.3  | 80.9       | 81.3  | 80.8  |
| 8/18/98 | 83.9                         | 83.5  | 84.2  | 85.8       | 85.9  | 85.3  |
| 8/19/98 | 85.4                         | 84.8  | 85.6  | 86.6       | 86.8  | 85.9  |
| 8/20/98 | 86.8                         | 86.7  | 86.9  | 88.0       | 88.0  | 87.6  |
| 8/24/98 | 82.6                         | 82.6  | 82.9  | 83.4       | 83.7  | 83.4  |
| 8/25/98 | 86.0                         | 86.6  | 87.0  | 86.9       | 86.8  | 87.0  |
| 8/26/98 | 84.7                         | 84.7  | 84.8  | 84.6       | 85.0  | 85.3  |
| 8/27/98 | 83.0                         | 82.1  | 82.1  | 82.7       | 82.2  | 82.3  |
| 8/28/98 | 83.7                         | 82.8  | 83.4  | 83.4       | 83.4  | 83.3  |
| 8/31/98 | 82.4                         | 81.6  | 82.1  | 82.2       | 82.1  | 82.3  |

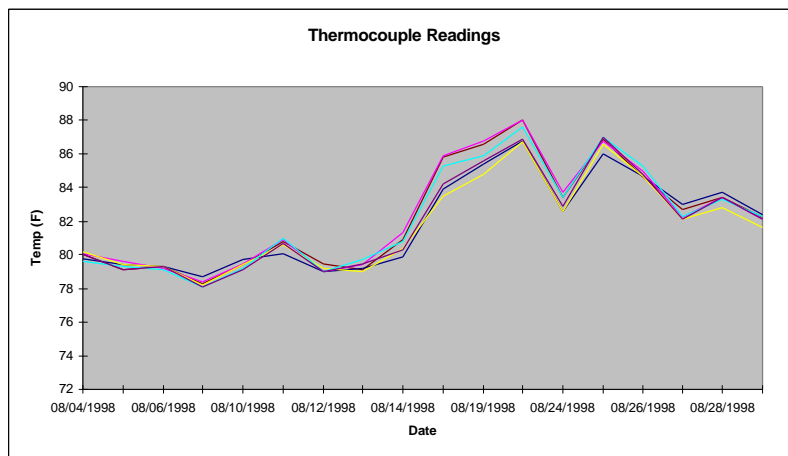


Figure B.4 Thermocouple Readings for ATL-98-1 Experiment

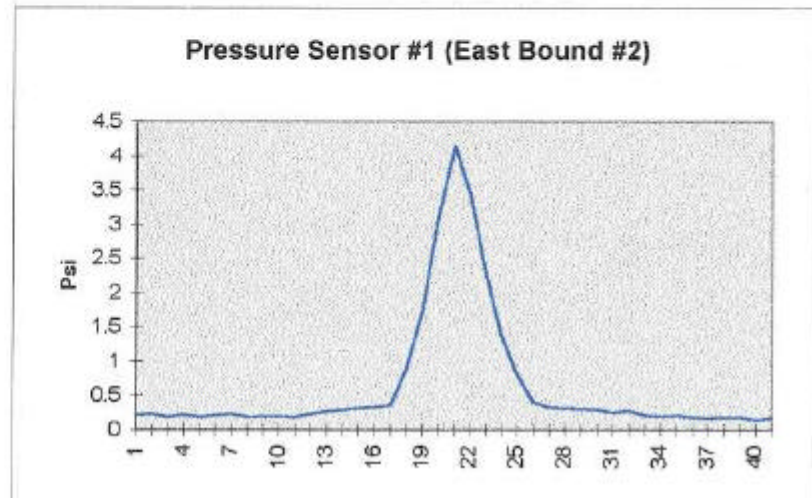
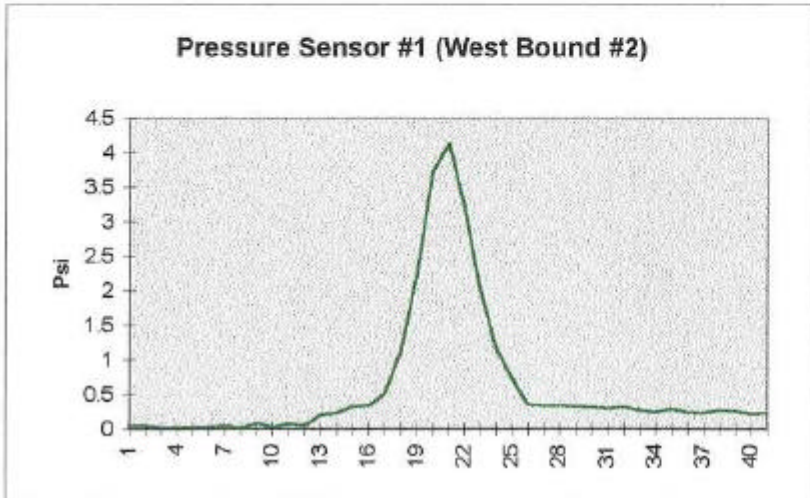
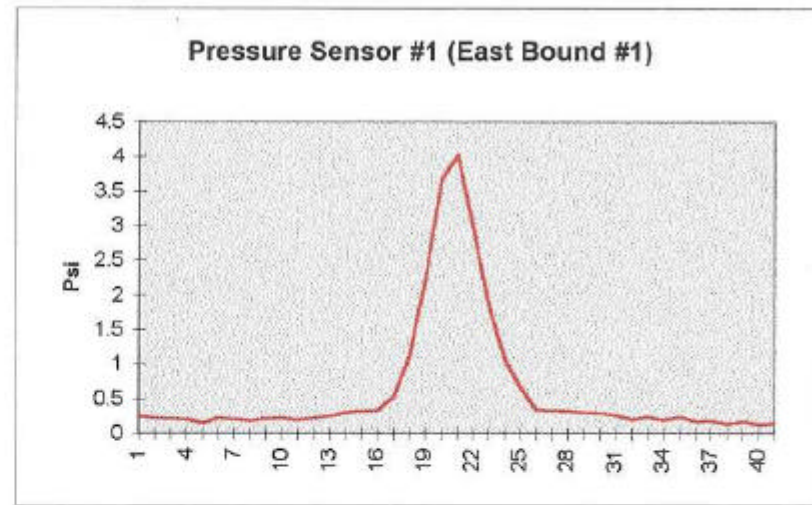
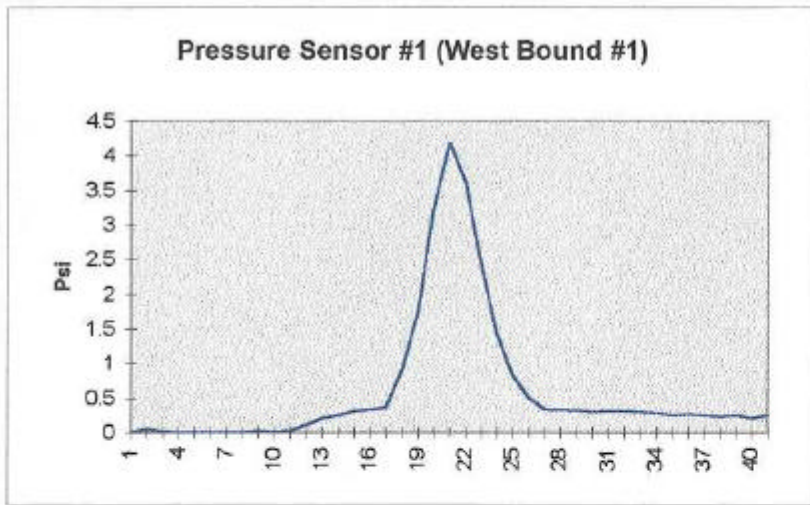


Figure B.5 Pressure Sensor Data at 1000 Load Repetitions for Pressure Sensor #1

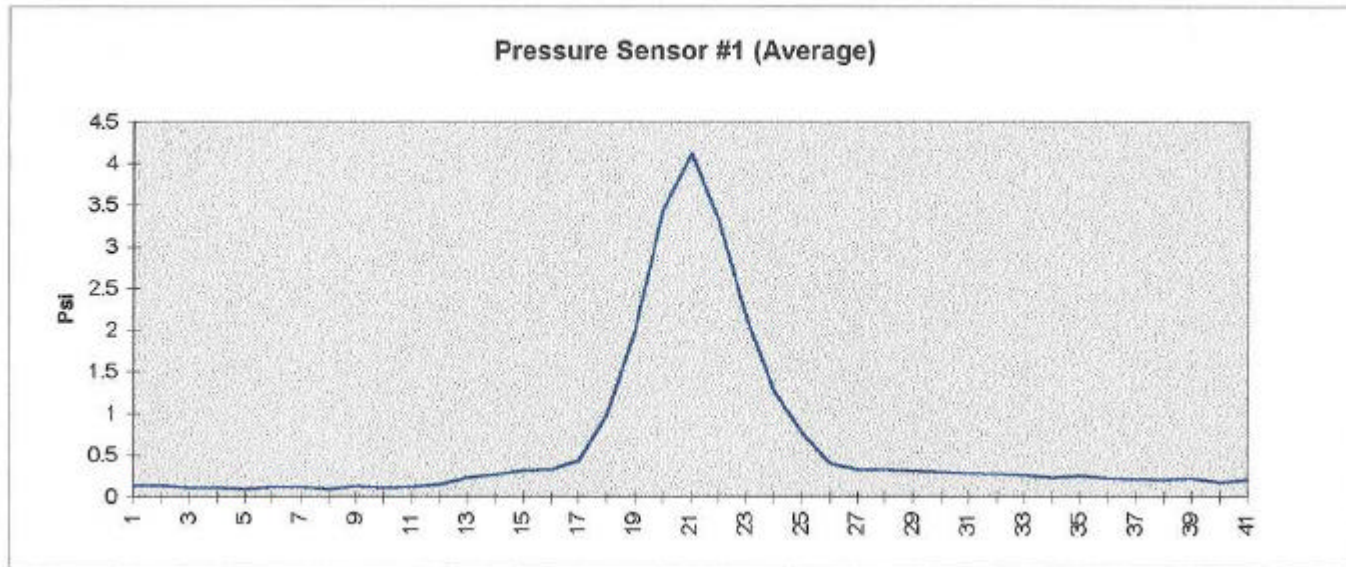


Figure B.6 Average Trace of Two Complete Cycles

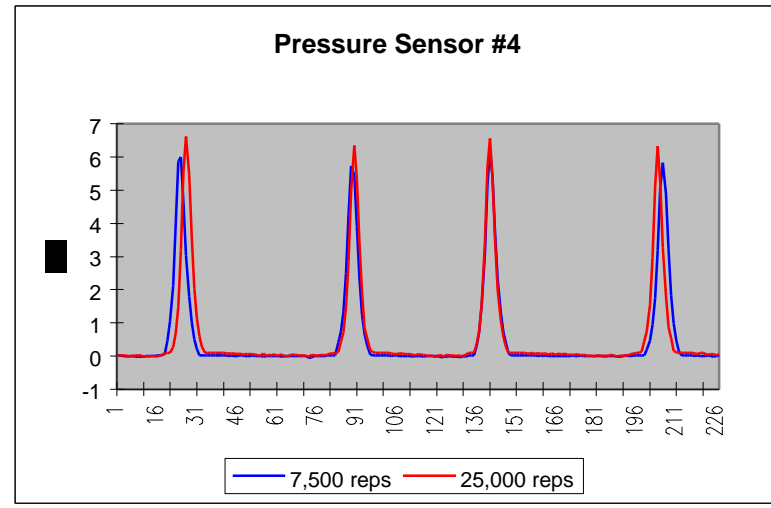
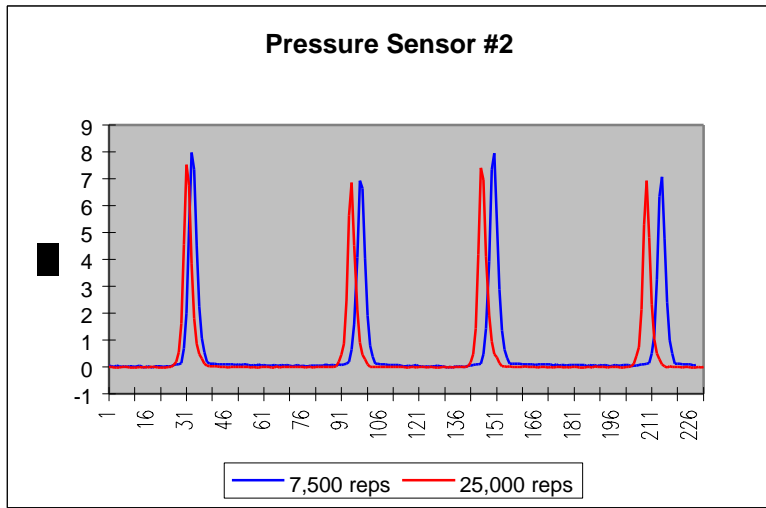
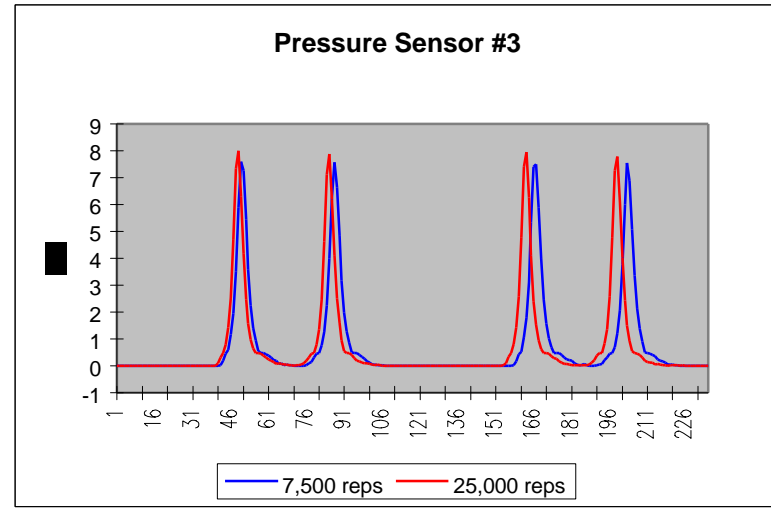
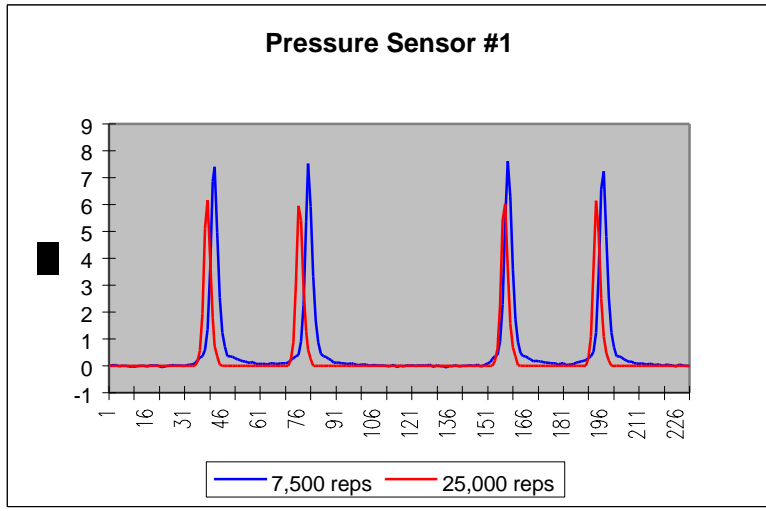


Figure B.7 Comparison of Pressure Between 7,500 and 25,000 Repetitions  
(Load Repetition at 18 kips)

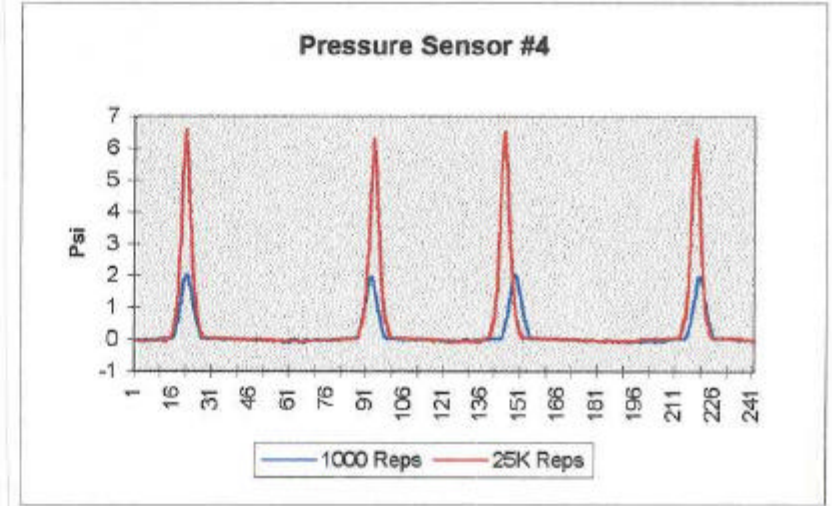
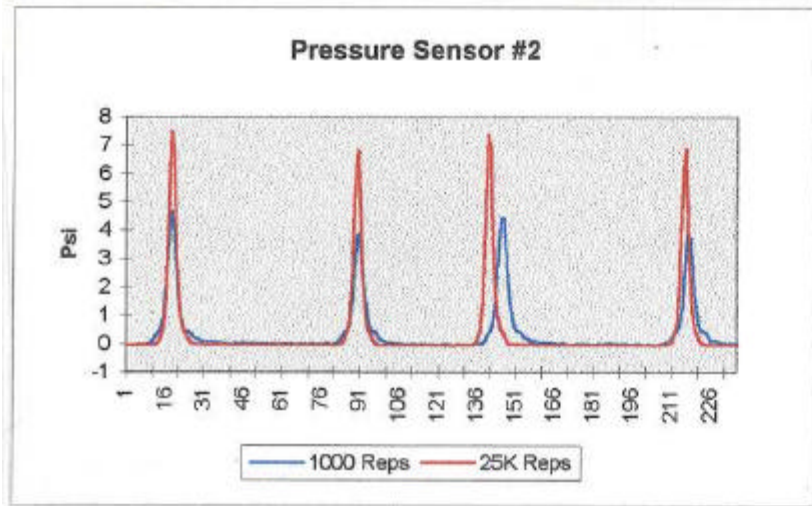
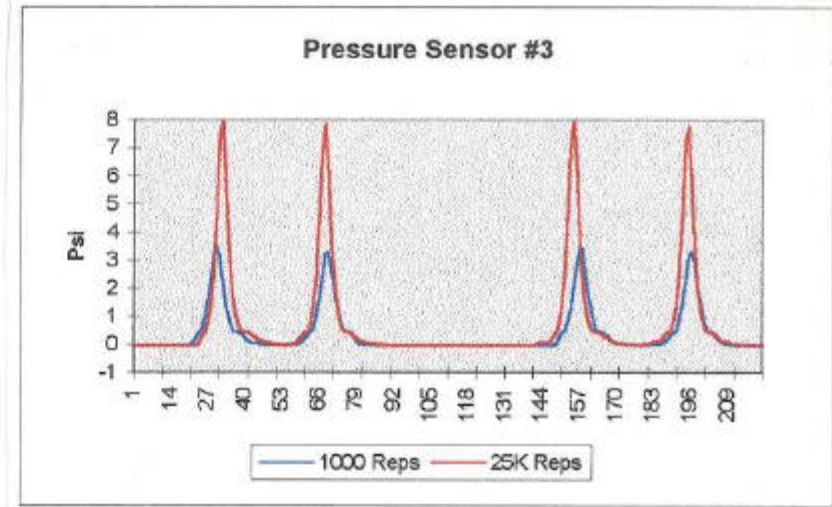
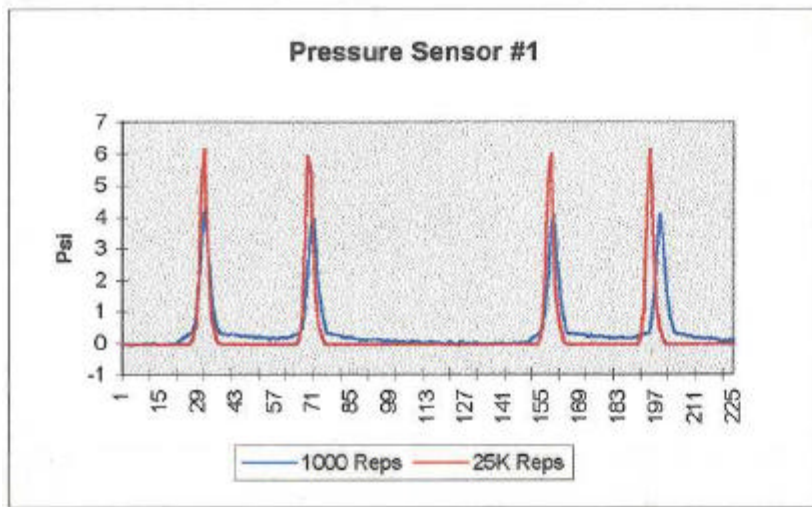


Figure B.8 Comparison of Pressure Between 1,000 and 25,000 Repetitions  
(1,000 Load Repetitions at 8 kips / 25,000 Load Repetitions at 18 kips)

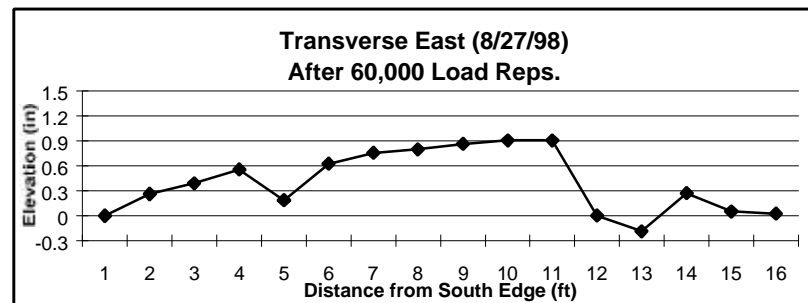
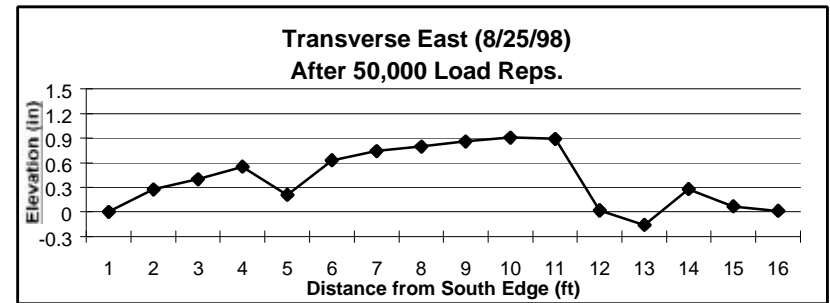
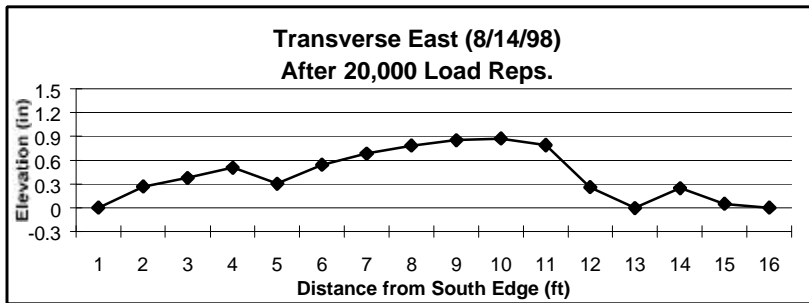
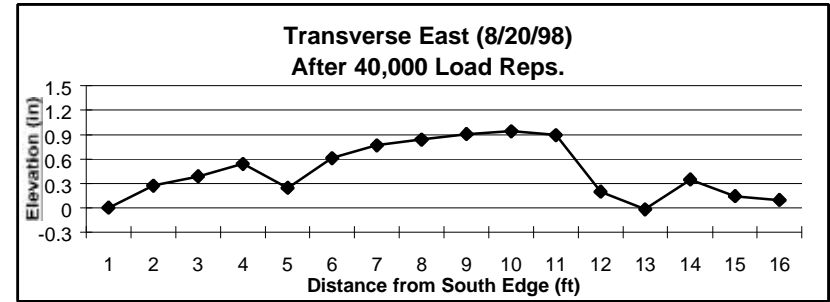
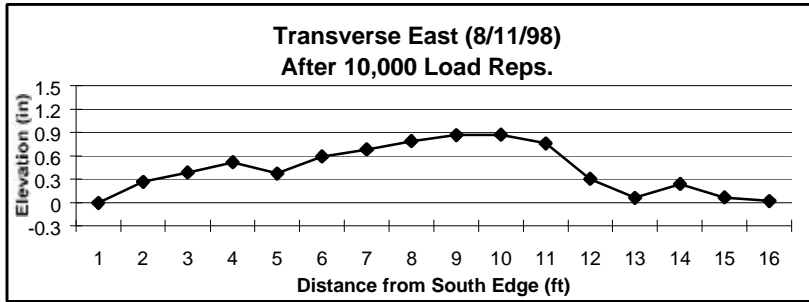
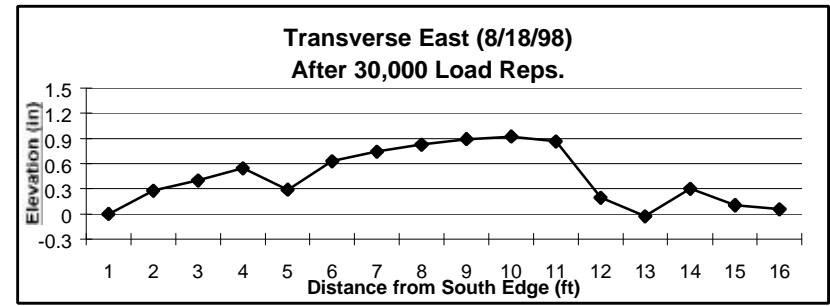
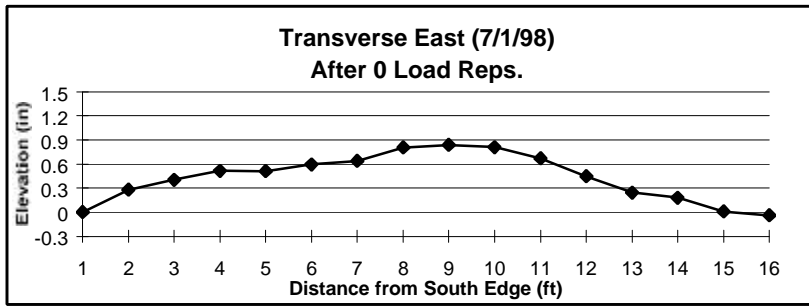


Figure B.9 Transverse Profiles (East)

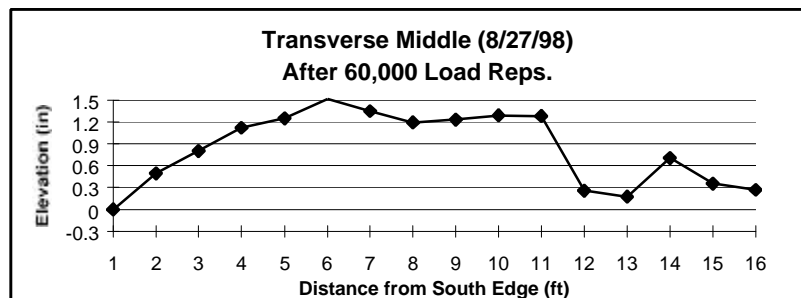
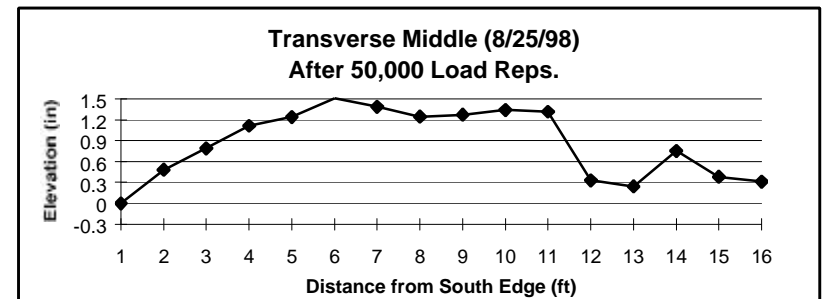
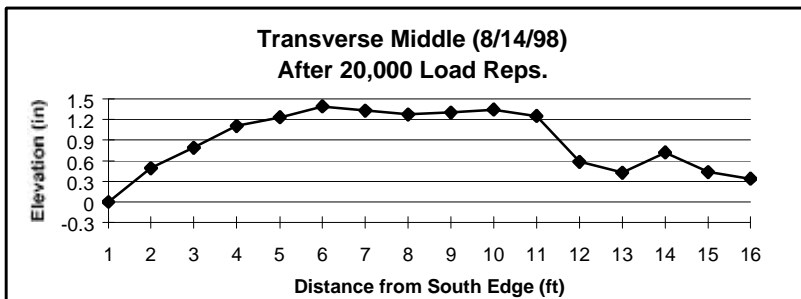
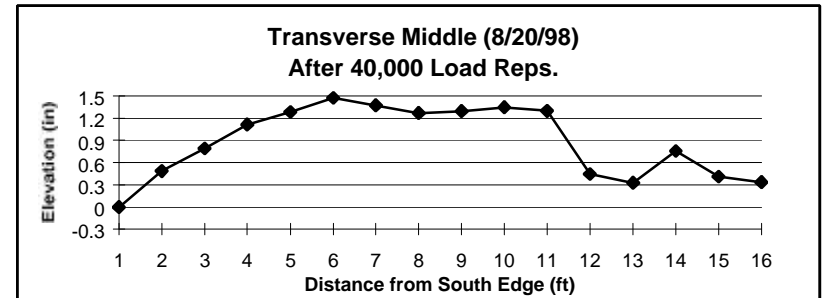
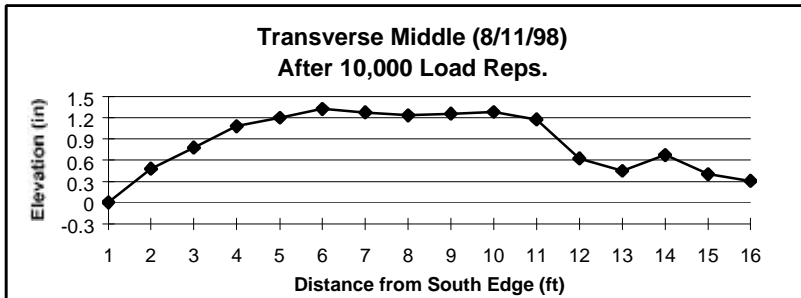
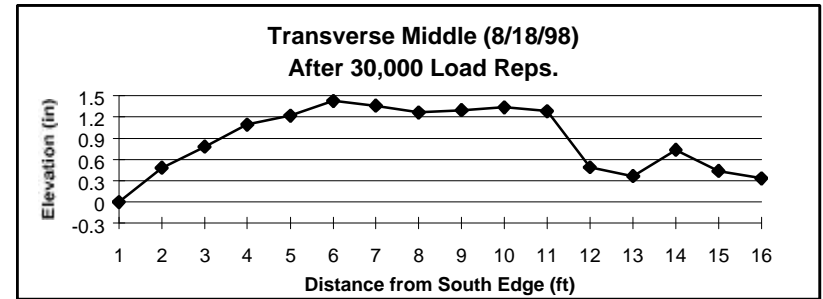
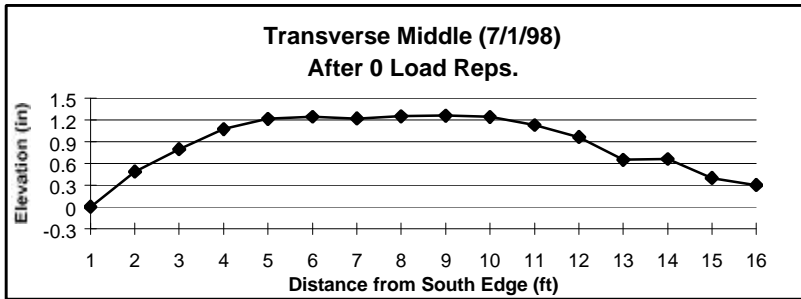


Figure B.10 Transverse Profiles (Middle)

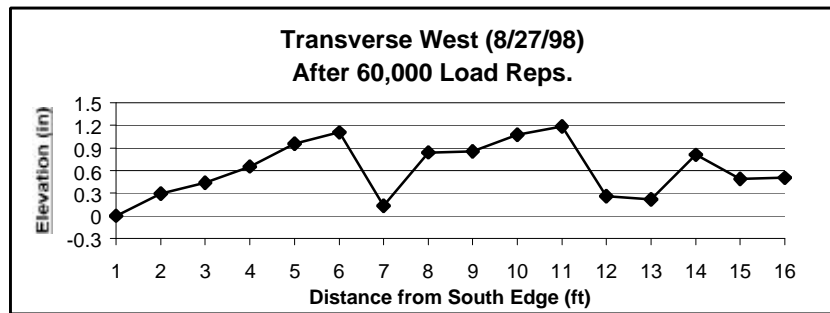
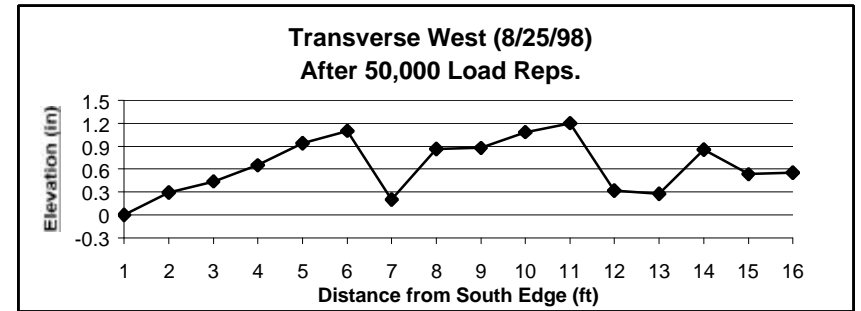
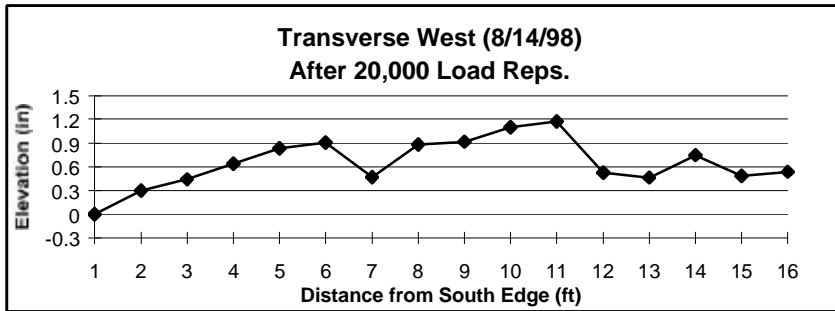
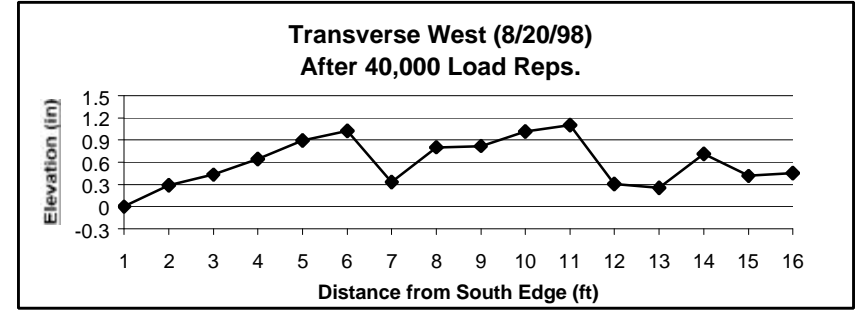
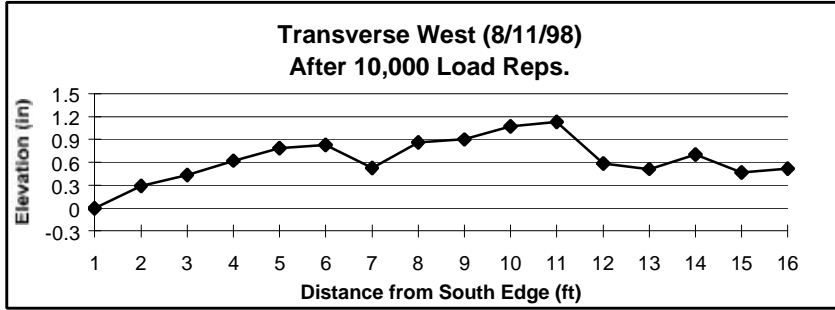
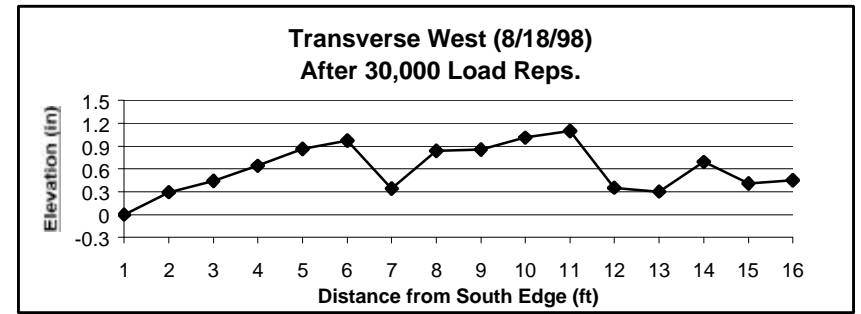
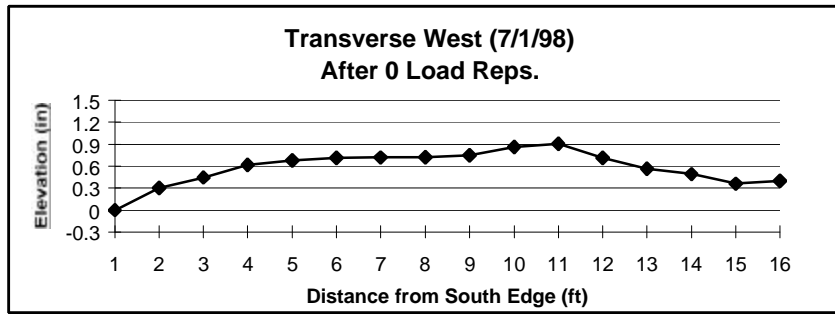


Figure B.11 Transverse Profiles (West)

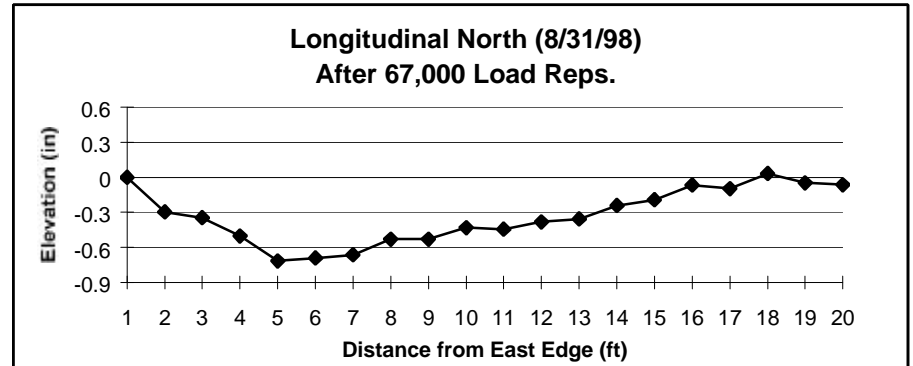
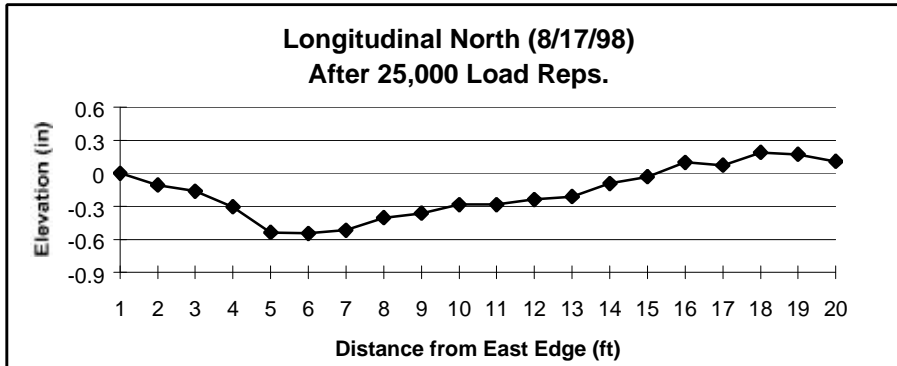
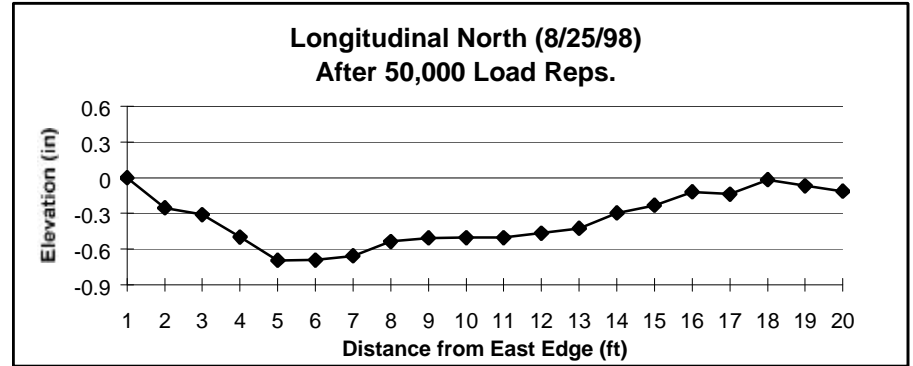
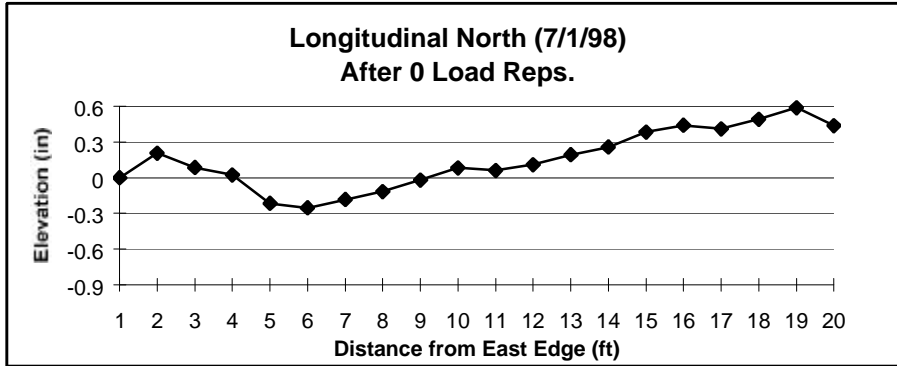


Figure B.12 Longitudinal Profiles (North Slab)

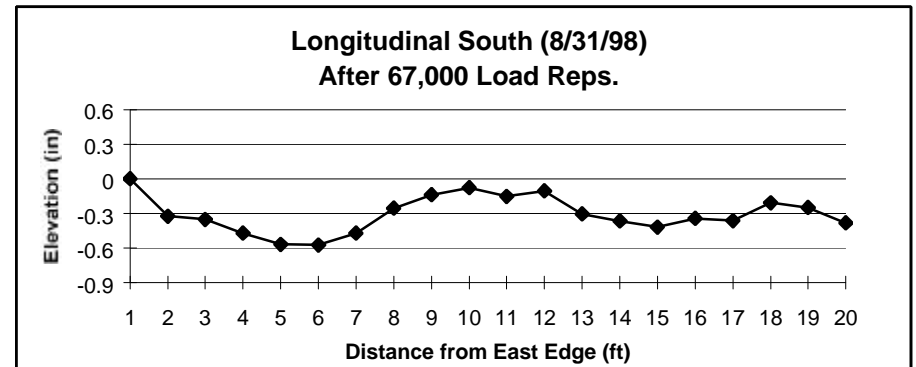
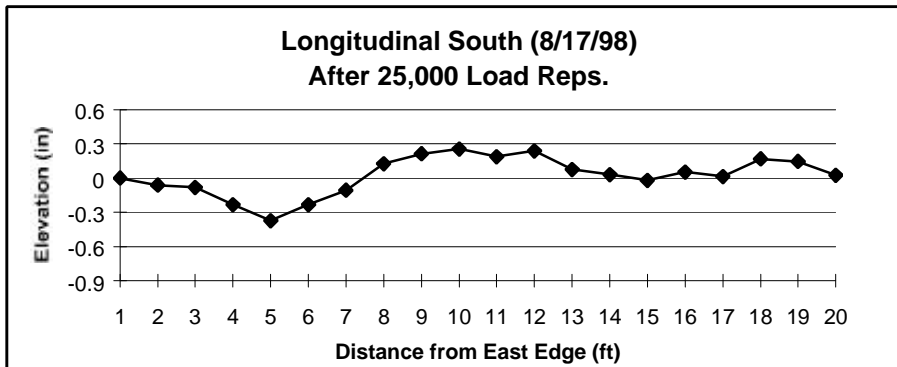
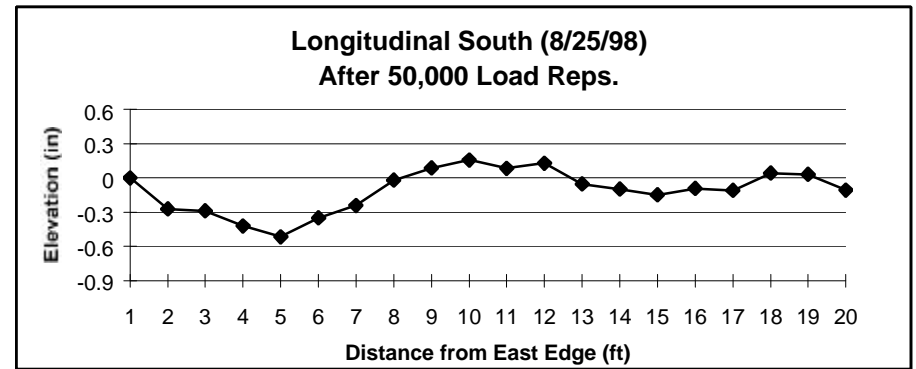
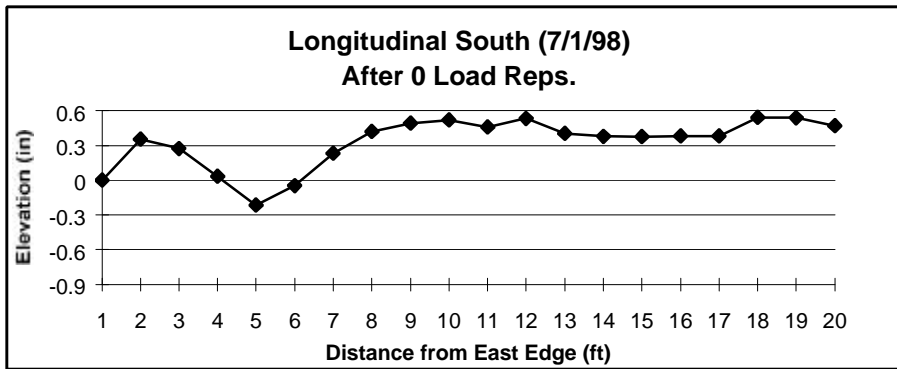


Figure B.13 Longitudinal Profiles (South Slab)

**APPENDIX C**

**SURFACE PROFILE FOR ATL-98-2 EXPERIMENT**

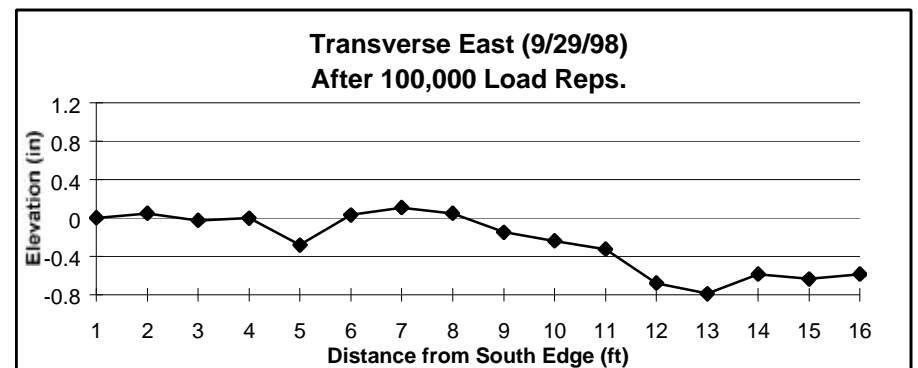
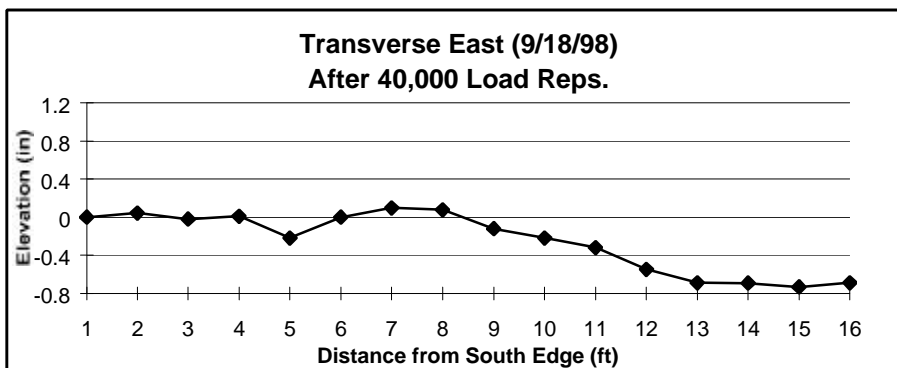
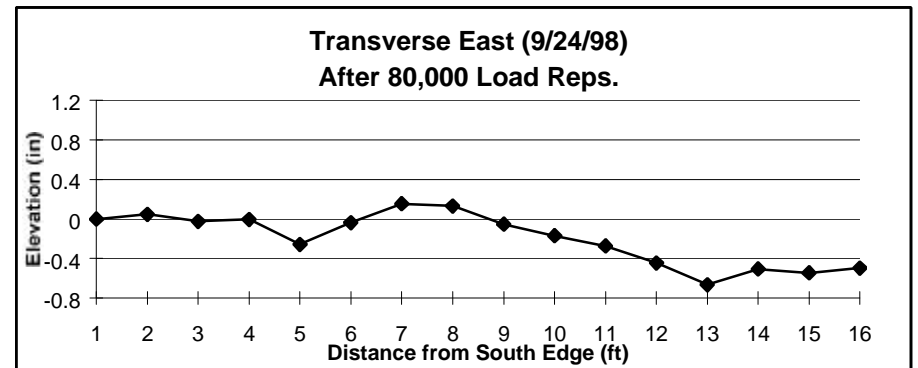
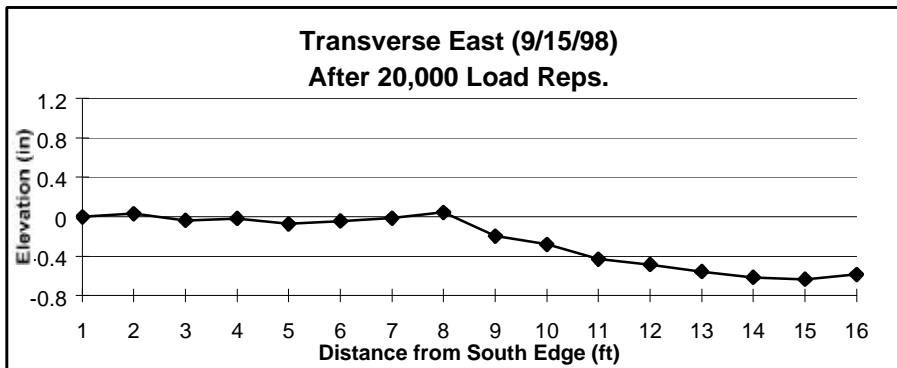
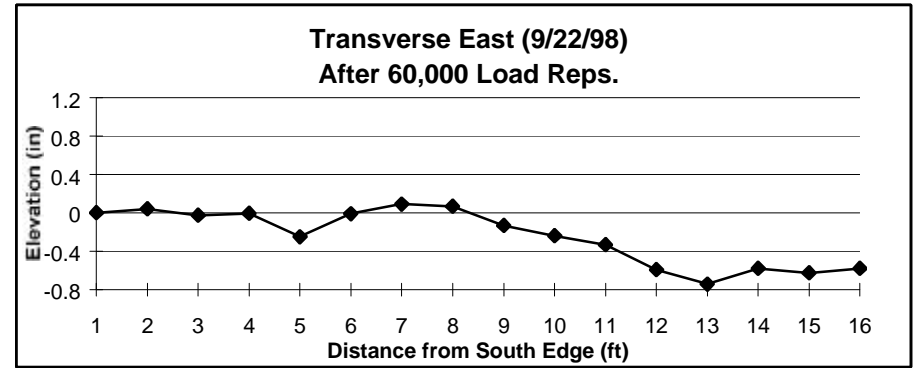
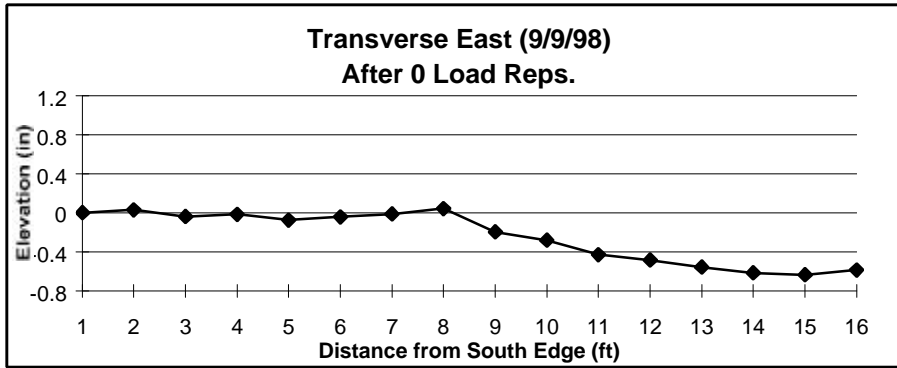


Figure C.1 Transverse Profiles (East)

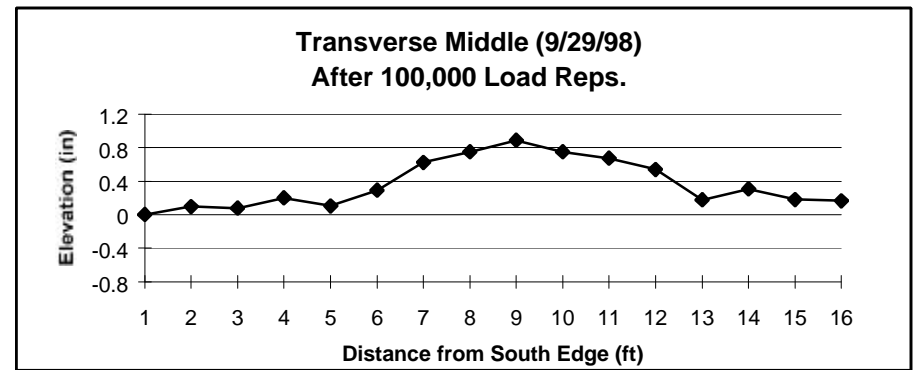
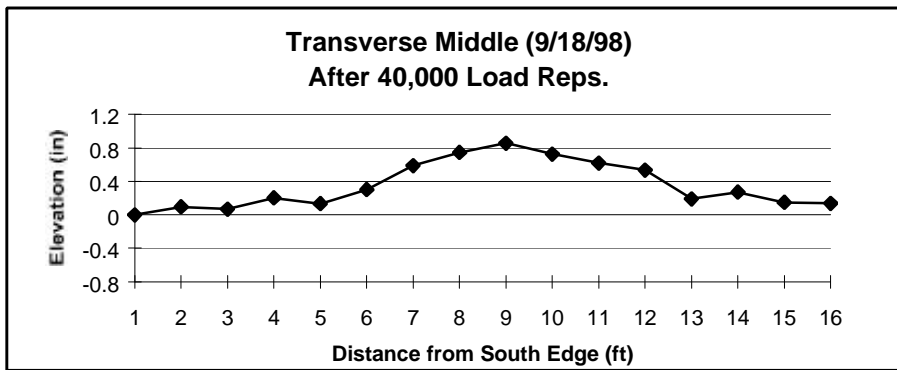
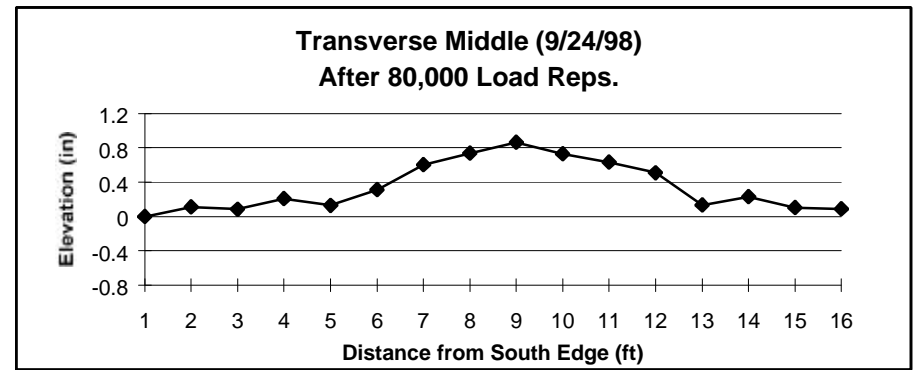
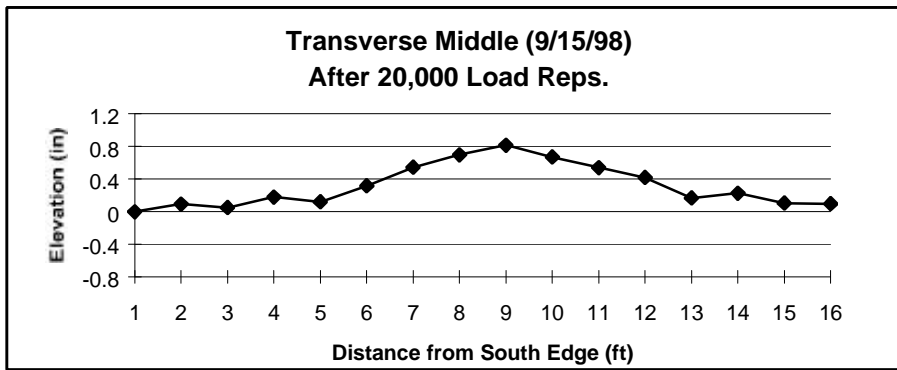
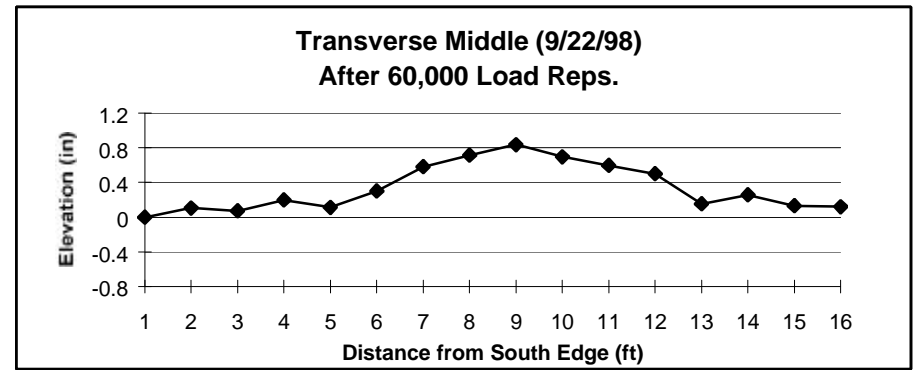
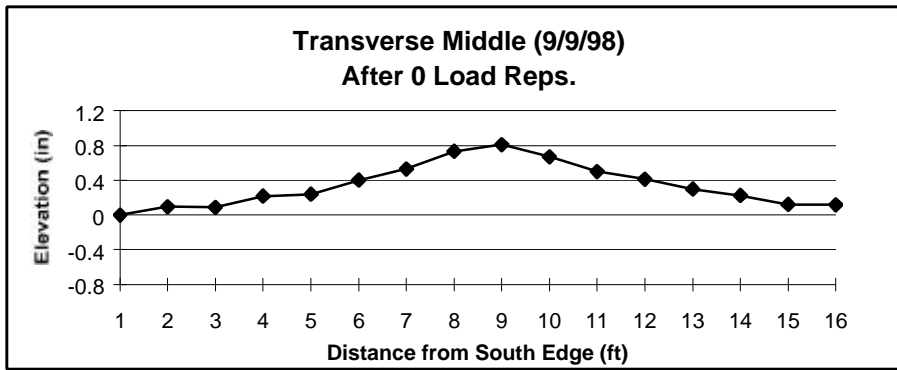


Figure C.2 Transverse Profiles (Middle)

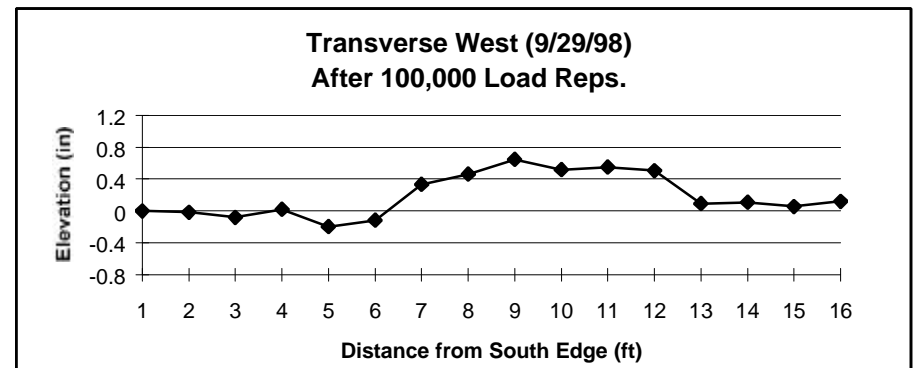
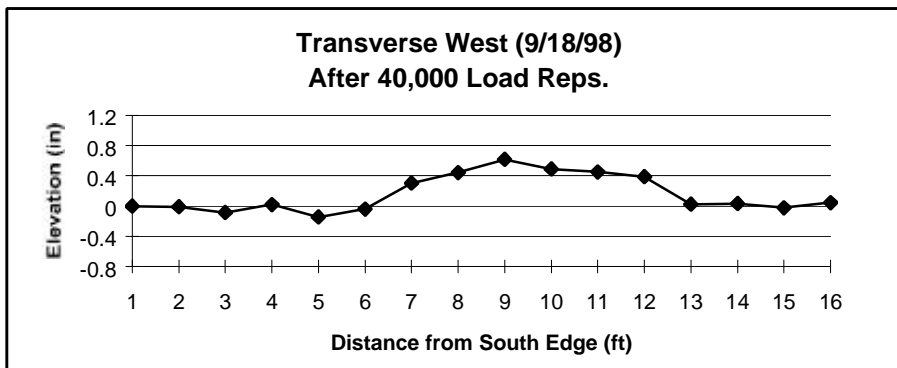
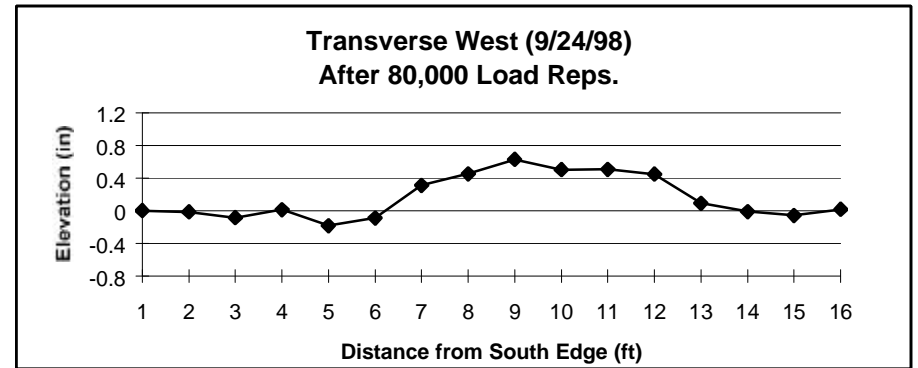
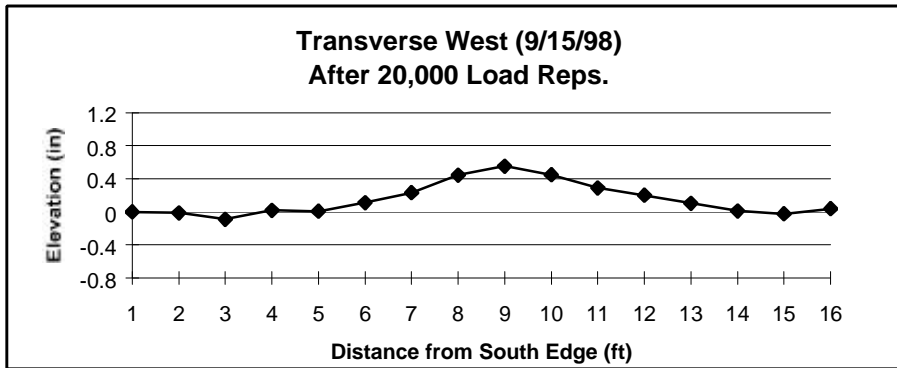
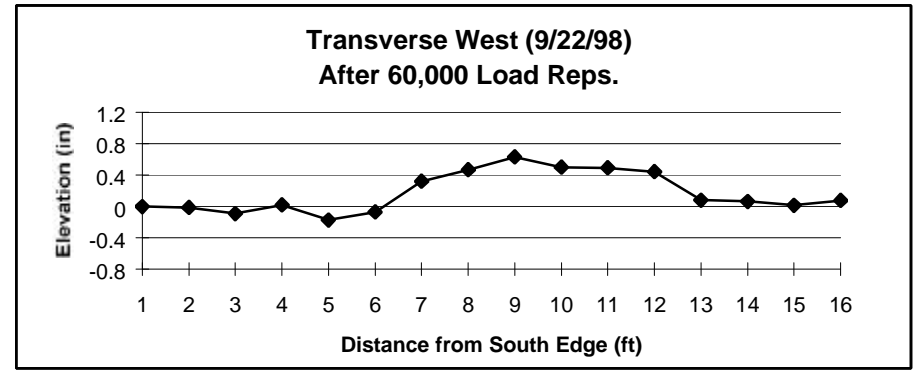
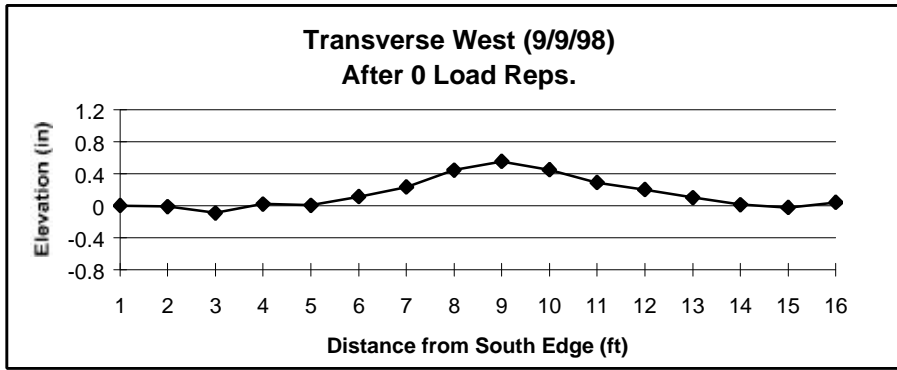


Figure C.3 Transverse Profiles (West)

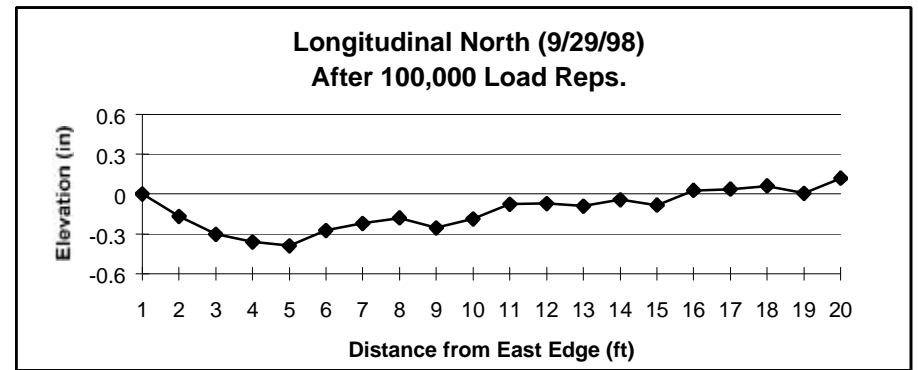
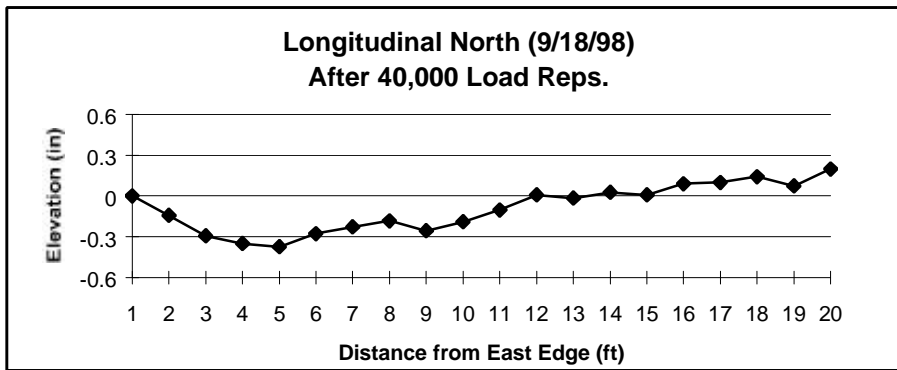
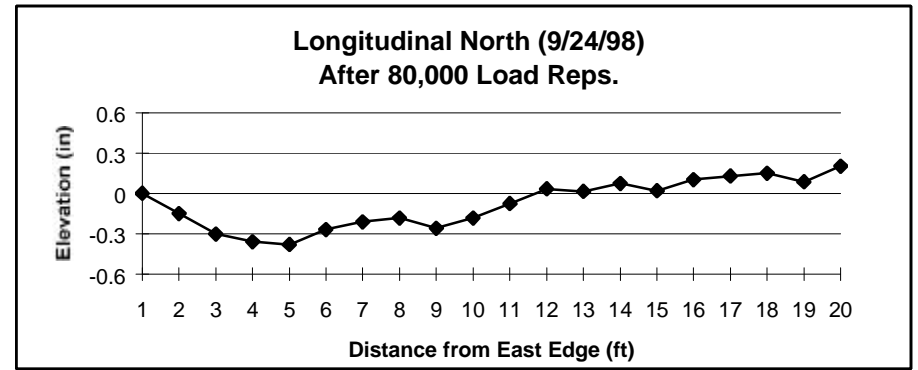
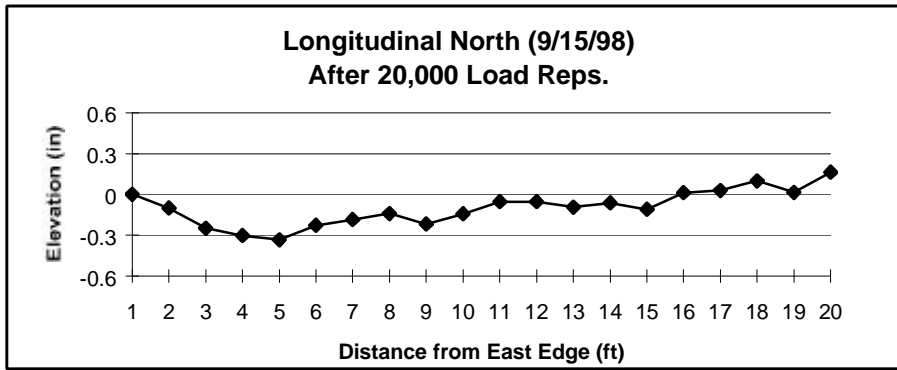
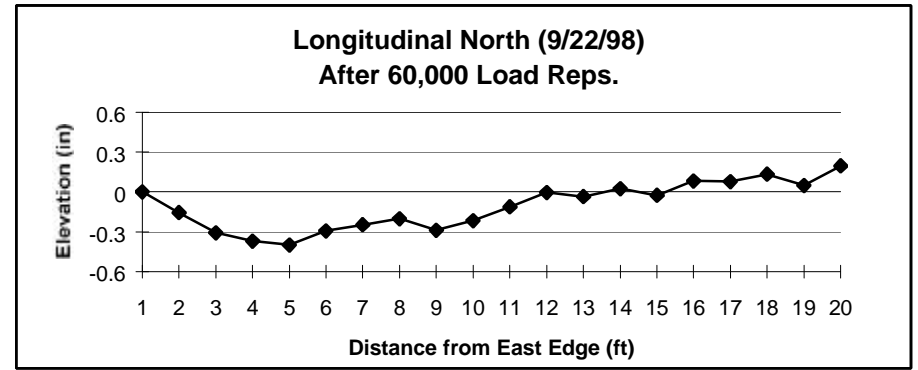
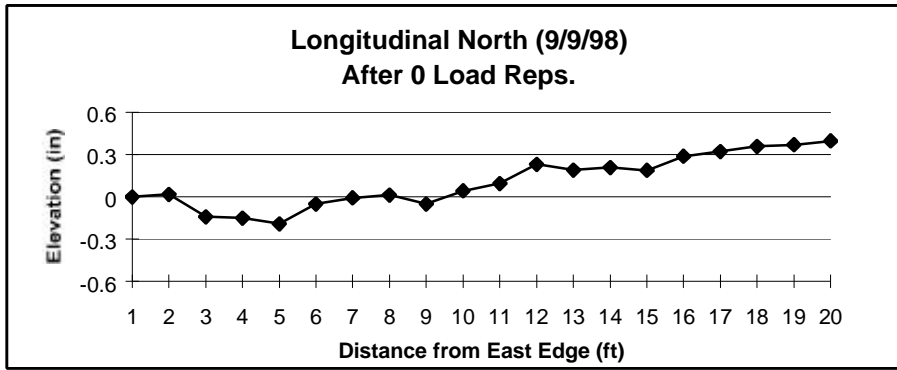


Figure C.4 Longitudinal Profiles (North Slab)

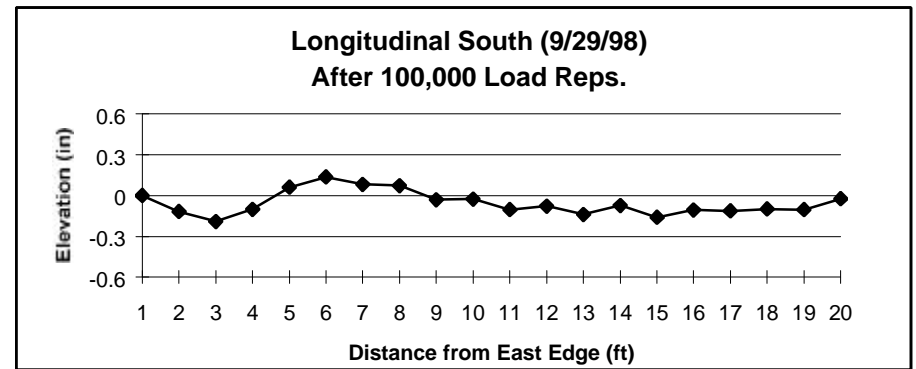
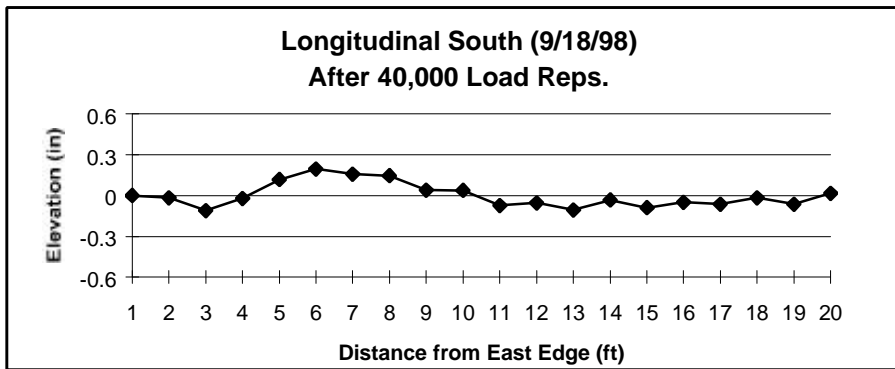
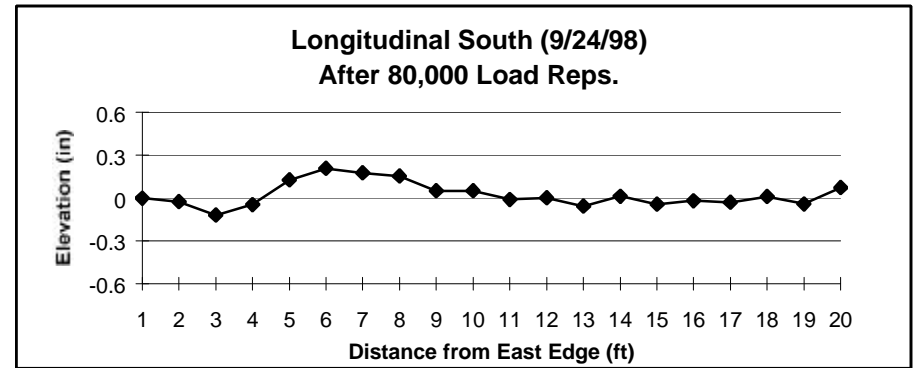
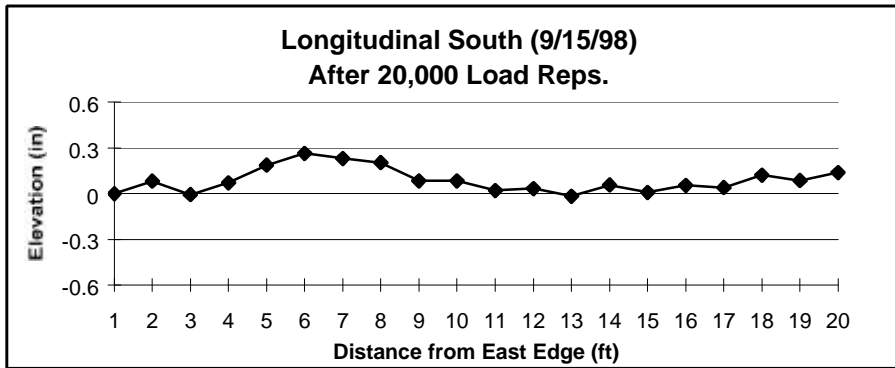
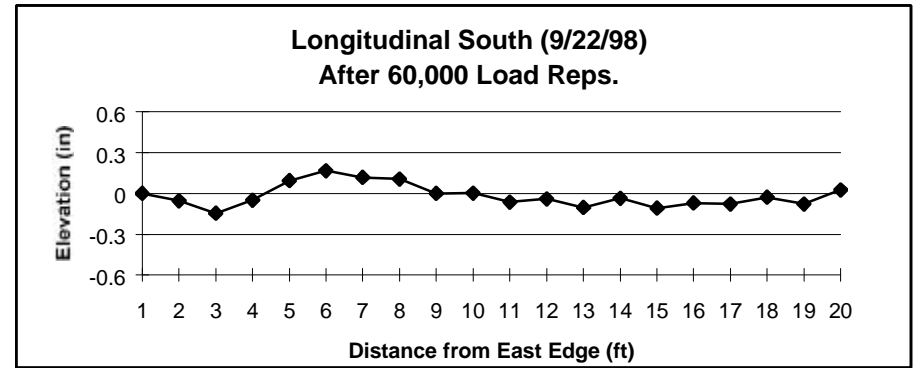
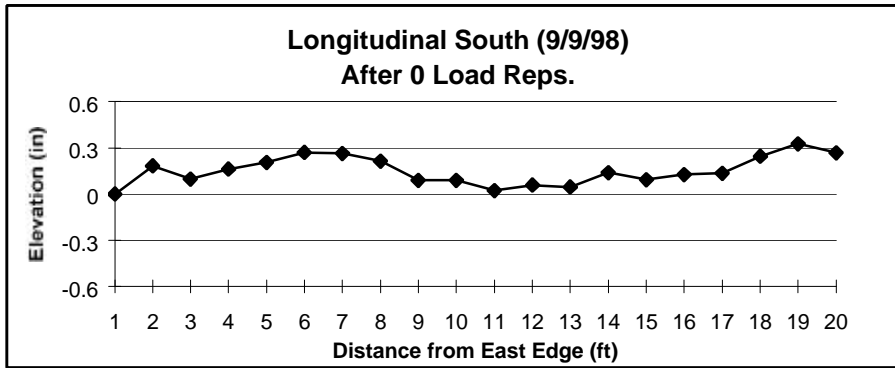


Figure C.5 Longitudinal Profiles (South Slab)

## References

Melhem, H.G., "Development of an Accelerated Testing Laboratory for Highway Research in Kansas," Final Report, Kansas Department of Transportation, Topeka, Kansas, November 1997, pp 65 (in print)

Porter, M., Hughes, W., Barnes, B., and Viswanath, K.P., "Non-Corrosive Tie Reinforcing and Dowel Bars for Highway Pavement Slabs," Final Report on Project HR-343, Iowa Department of Transportation, November 1993.

Porter, M. and Braun, R.L. "Summary of Glass Fiber Reinforced Plastic Dowel Bar Research at Iowa State University," Engineering Research Institute, Iowa State University, June 1996.

Sargand, S., Hazen, G., Khoury, I., Pannila, I., and Rogers, R., "Evaluation of Pavement Joint Performance," Final Report for Job No. 14474(0), Center for Geotechnical and Environmental Reserach, Ohio University, January 1994.

White, T.D., and Hua, J. "Relating Accelerated Pavement Testing to In-service Pavement Performance," Proceedings of the Fifth International Conference on Bearing Capacity of Roads and Airfields (BCRA'98), Norwegian University of Science and Technology, Trondheim, Norway, July 6-8, 1998, Vol. 2, pp 783-792.

Baker, H.B., Buth, M.R., and Van Deusen, D.A. "Minnesota Road Research Project Load Response Instrumentation Installation and Testing Procedures," Report No. MN/PR-94/01, Minnesota DOT, St. Paul, Minnesota, March 1994.

Van Deusen, D.A., Newcomb, D.E., and Labuz, J. F. "A Review of Instrumentation Technology for the Minnesota Road Research Project," Report No. FHWA/MN/RC-92/10, Minnesota DOT, St. Paul, Minnesota, April 1992.

Heck, J., and Piau, J., Gramsammer, J.C., Kerzreho, J.P., and Odeon, H. "Thermo-visco-elastic Modeling of Pavements Behaviour and Comparison with Experimental Data from LCPC Test Track," Proceedings Fifth International Conference on Bearing Capacity of Roads and Airfields (BCRA'98), Norwegian University of Science and Technology, Trondheim, Norway, July 6-8, 1998, Vol. 2, pp 763-772.

Ullidtz, P., and Ekdahl, P. "Full-Scale Testing of Pavement Response," Proceedings of the Fifth International Conference on Bearing Capacity of Roads and Airfields (BCRA'98), Norwegian University of Science and Technology, Trondheim, Norway, July 6-8, 1998, Vol. 2, pp 857-866.

HITEC (1998). *Evaluation Plan for Fiber Reinforced Polymer Composite Dowel Bars and Stainless Steel Dowel Bars.*